Chapter 7

Neural Network Model and Controller in
Nonlinear Internal Model Control

This chapter presents the capabilities of neural network to learn the forward and inverse model of the simulated continuous stirred tank reactor in order to represent plant model and controller, respectively. Then both models are implemented in the Nonlinear Internal Model Control (NIMC) configuration. The control performance of the NIMC is tested and compared with that of the GMC.

7.1   Nonlinear Internal Model Control

In this work, nonlinear neural networks replace both the internal model and the controller in the Internal Model Control (IMC) structure. The internal model is replaced by a neural network model of the forward process dynamics (referred to here a neural network forward model), which uses to predict the output of the process given past values of control actions and the process output predictions. The controller is replaced by a neural network model of the inverse of the process dynamics (referred to here as the neural network inverse model), which is trained to computed the manipulated variable action given the past and current errors and the past control actions. Since the process model and the model inverse are represented with two different neural networks trained independently, the product of the steady state gains of the process model and the model inverse may not be unity, therefore it may cause steady state offset in a controlled variable.

In this work the NIMC is utilized to control the reactor temperature of the Continuous Stirred Tank Reactor (CSTR) by manipulating the coolant feed temperature. The control performance of the NIMC is tested in the same fashion as those used to test the control performance of the GMC. Simulated data of the CSTR are employed to identify the neural network forward and inverse model of the system.

7.2 Neural Network Forward Modeling

Mathematical models of the continuous stirred tank reactor presented in the previous chapter are employed to generate the data for training, cross validation and testing the neural network forward model. These data are also utilized to train, cross validate, and test the neural network inverse model, which will be proposed in the next section. The multilayer feedforward network representing the forward model of the CSTR is composed of five input nodes, seven hidden nodes and one output node.

The forward model expressed as the function of current and two past values of the coolant feed temperature and two past value of the reactor temperature are as follows:

$$T(t+1) = f\big(T(t), T(t-1); T_{cf}(t), T_{cf}(t-1), T_{cf}(t-2)\big) \qquad (7.1)$$

The neural network structure representing the forward model of the CSTR and the modeling results are shown in Figure 7.1-7.4.
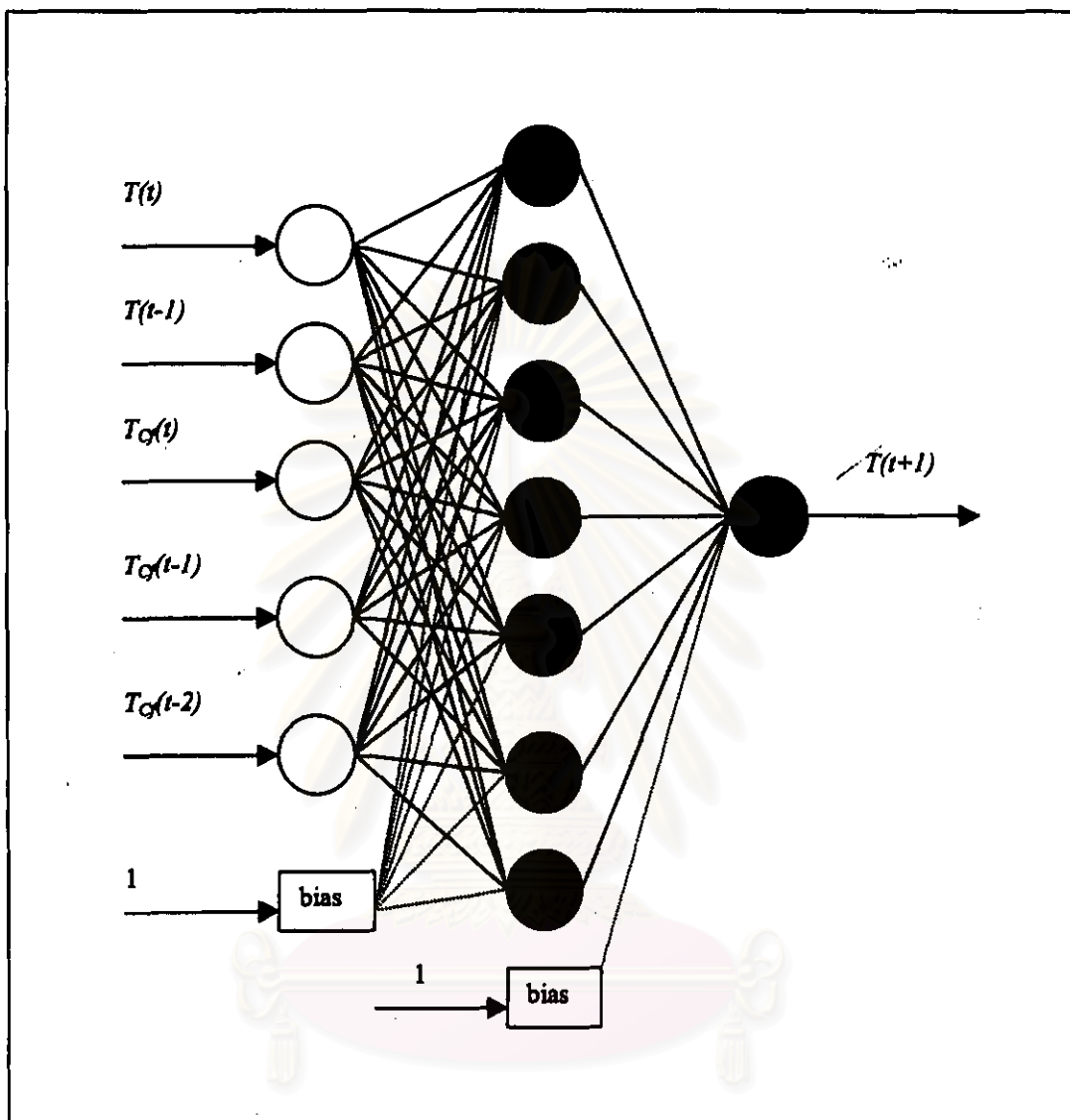
Figure 7.1: Neural network architecture representing the forward model of the CSTR.
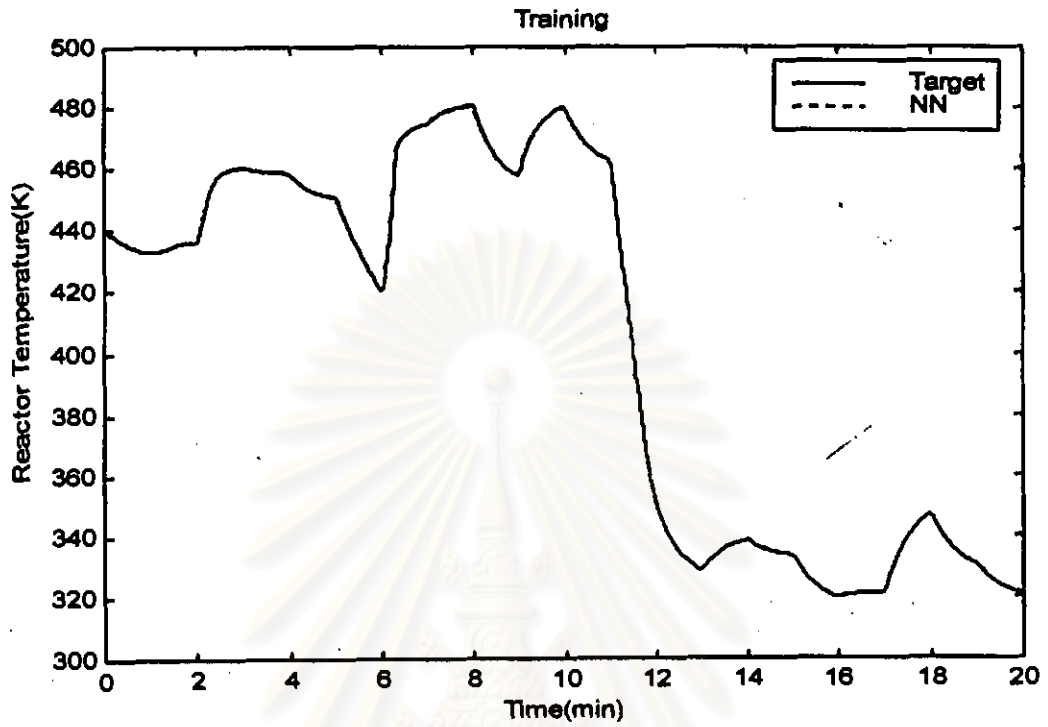
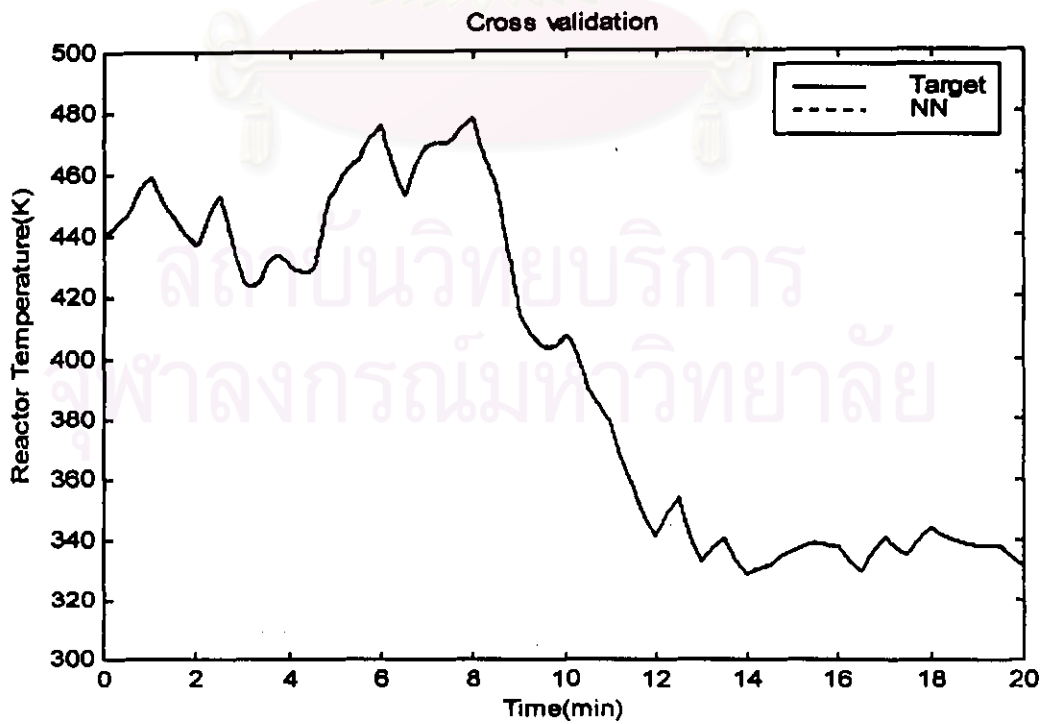Figure 7.2: Neural network forward modeling of CSTR: Training result

Figure 7.3: Neural network forward modeling of CSTR: Cross validation result.
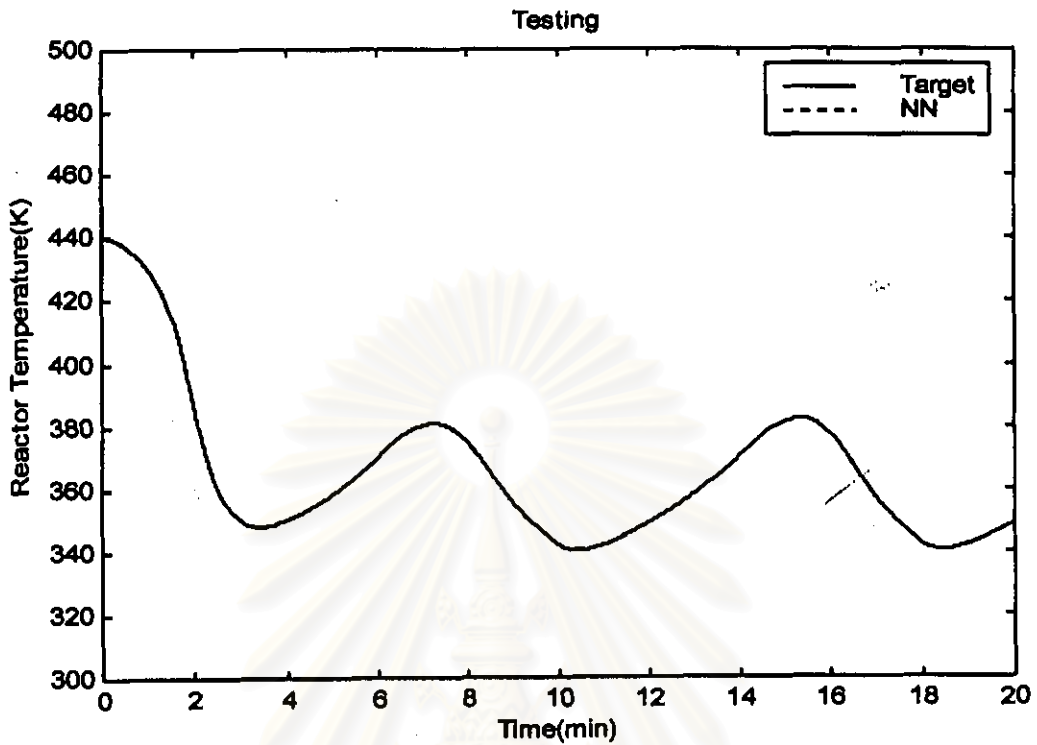
Figure 7.4: Neural network forward modeling of CSTR: Testing result.

7.3 Neural Network Inverse Modeling

The multilayer feedforward network representing the inverse model of the CSTR is composed of five input nodes, six hidden nodes and one output node. The inverse model expressed as the function of current and past values of inputs and output are as follows:

$$T_{Cf}(t) = f^{-1}\left(T(t+1), T(t), T(t-1); T_{Cf}(t-1), T_{Cf}(t-2)\right) \quad (7.2)$$

Note that a future value of the output ($T(t+1)$) is required in equation (7.2). During training, this value is available from the plant input-output data, but when the controller is implemented in a closed loop, it is not available. Thus, a predicted value $\hat{T}(t+1)$ must be used instead. Under the assumption that the feedback controller is the exact inverse of the neural network forward model, the IMC error, $e(t)$, may be used in place of $\hat{T}(t+1)$. Thus,

$$T_{Cf}(t) = f^{-1}\big(e(t), T(t), T(t-1); T_{Cf}(t-1), T_{Cf}(t-2)\big) \qquad (7.3)$$

where $e(t) = T^{sp}(t) - (T(t) - \hat{T}(t))$. The control performance of the nonlinear internal model control is tested in the same cases as those employed to test the GMC. The neural network structure representing the inverse model of the CSTR and its modeling results are demonstrated in Figure 7.5-7.8. After the forward and the inverse model are obtained, they are implemented in NIMC configuration as demonstrated in Figure 7.9. However small offsets exist in some case studies because of the existence of the model errors and the lack of the exact inverse model then PI controller is added to such configuration in order to remove the offsets as shown in Figure 7.10.
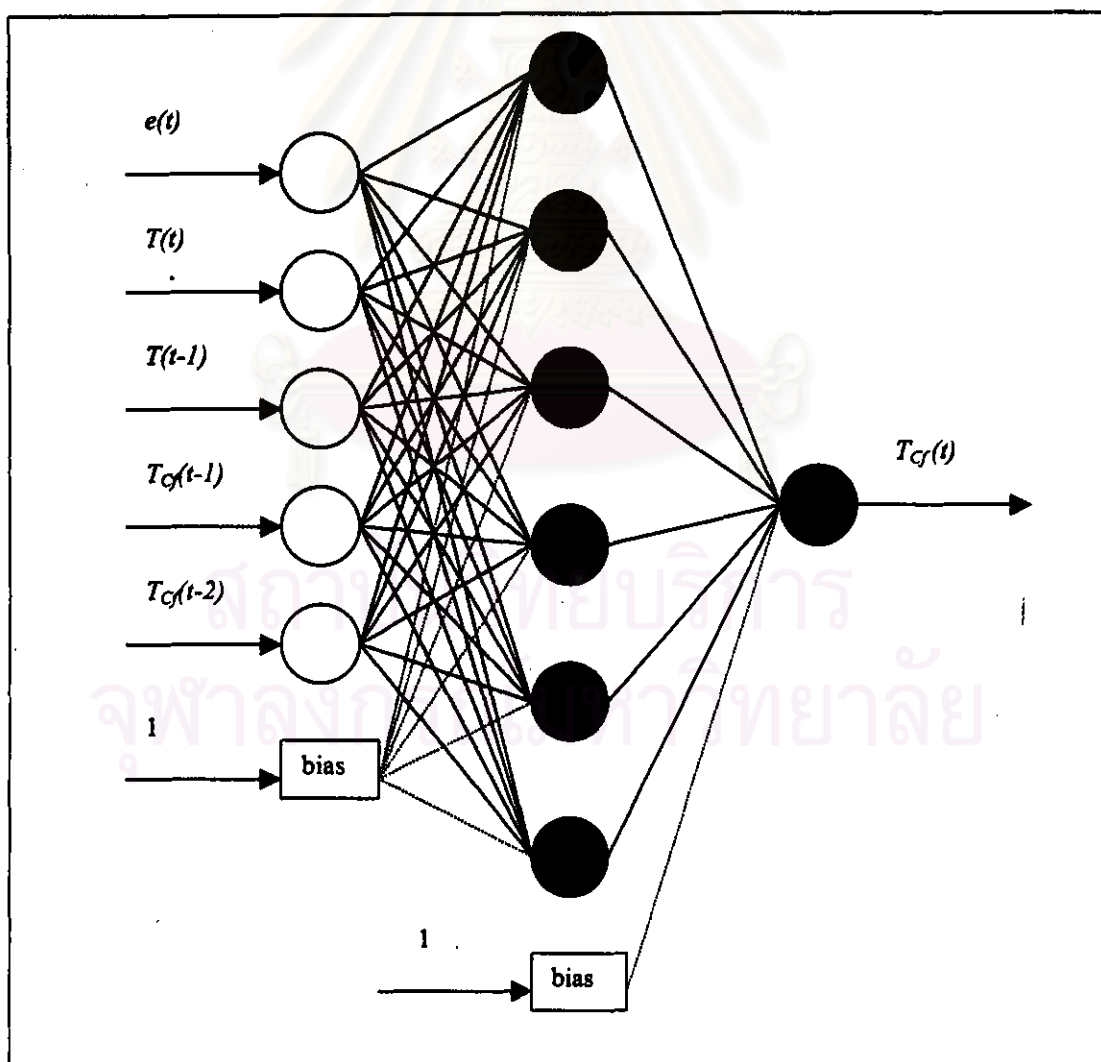

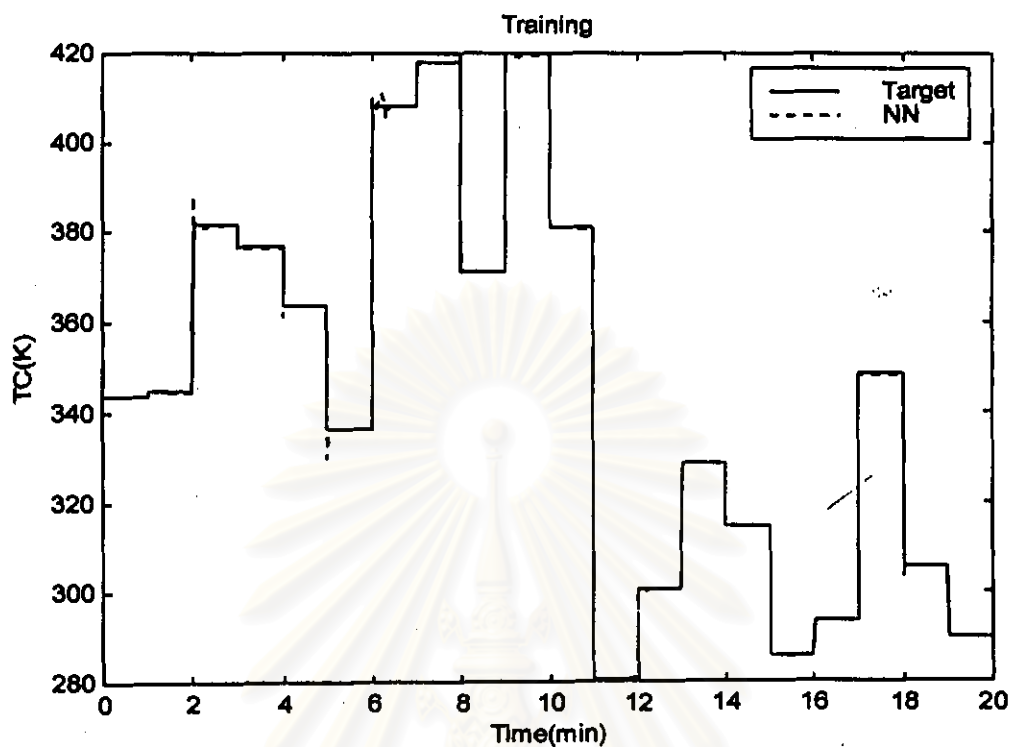Figure 7.5: Neural network architecture representing the inverse model of the CSTR.

Figure 7.6: Neural network inverse modeling of CSTR: Training result.
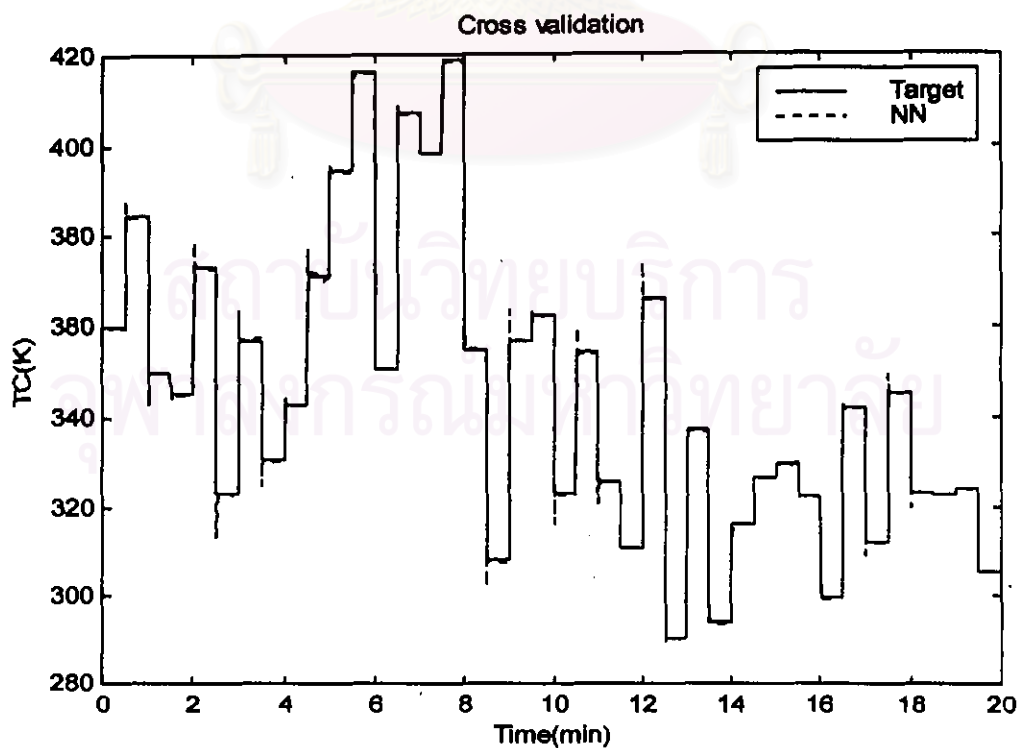

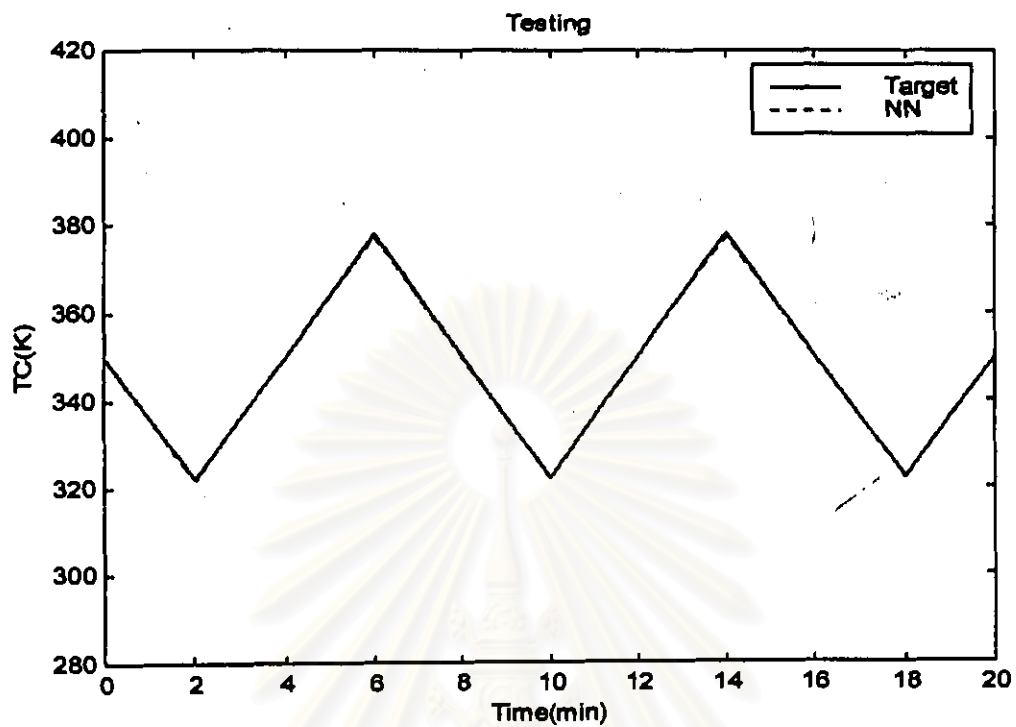Figure 7.7: Neural network inverse modeling of CSTR: Cross validation result.

Figure 7.8: Neural network inverse modeling of CSTR: Testing result.
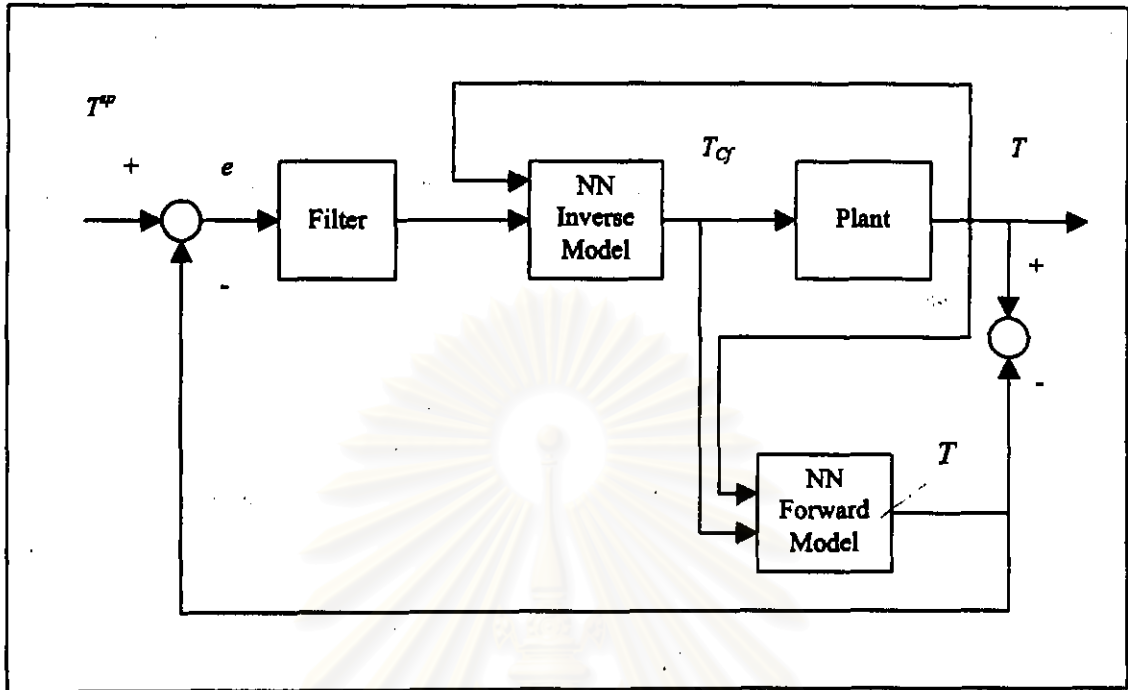
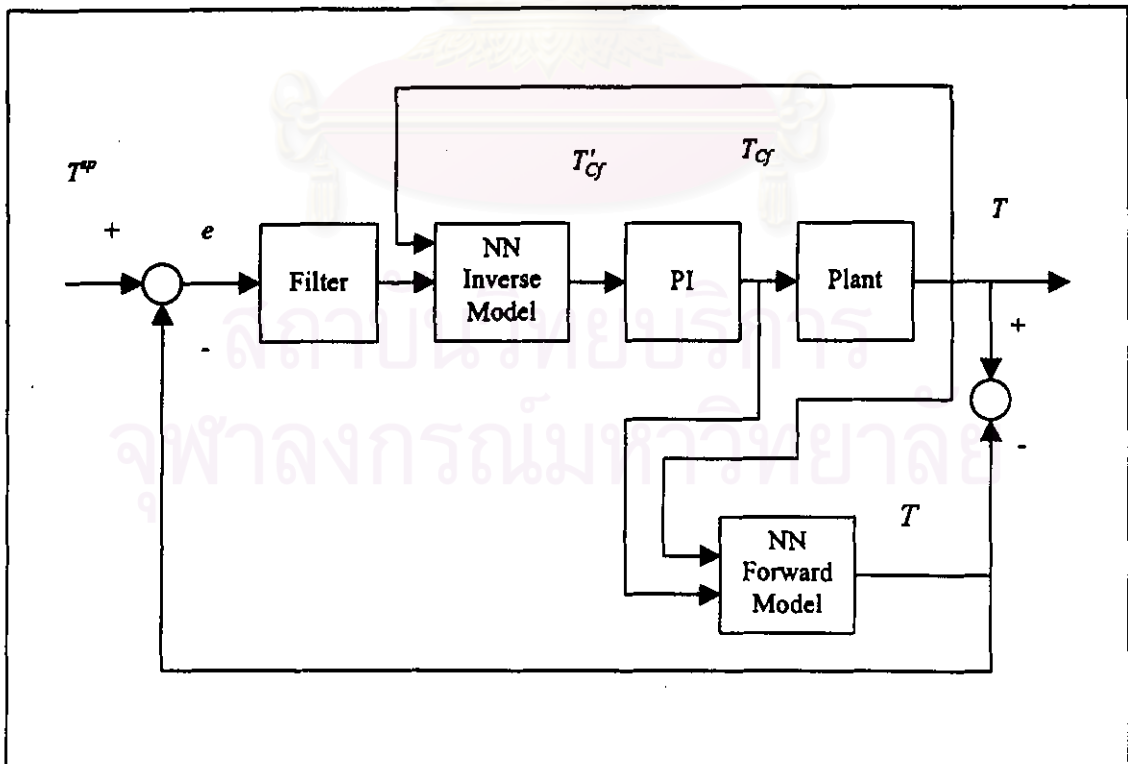Figure 7.9: Nonlinear internal model control configuration.

Figure 7.10: Proposed nonlinear internal model configuration.

Table 7.1: Comparison of the GMC-NN, the NIMC-PI, and the PI control performance

| Robustness Tests	Performance Tests	IAE		
		GMC-NN	NIMC-PI	PI
Nominal condition				
1. no change in parameters	10% T_f	1.3165	5.0519	4.1567
2. no change in parameters	10% C_{Af}	0.6342	1.7366	2.5866
Plant-model mismatches				
3. 20% ko	10% T_f	1.5472	5.9969	4.1379
4. 20% ko	10% C_{Af}	0.7442	2.2985	2.5255
5. −50% hA	10% T_f	2.4230	6.2272	4.6818
6. −50% hA	10% C_{Af}	1.4328	2.2968	3.1155
7. 10% Hr	10% T_f	3.4525	11.3668	6.8469
8. 10%(-ΔH)	10% C_{Af}	1.4743	5.9255	6.2419
Nominal condition				
9. no change in parameters	change T^{sp} to 450K	7.1156	1.6419	2.0615
Plant-model mismatches				
10. 20% ko	change T^{sp} to 450K	7.1266	1.3149	1.3656
11. −50% hA	change T^{sp} to 450K	6.1852	1.3854	2.1550
12. 10%(-ΔH)	change T^{sp} to 450K	6.2646	1.0764	2.8675
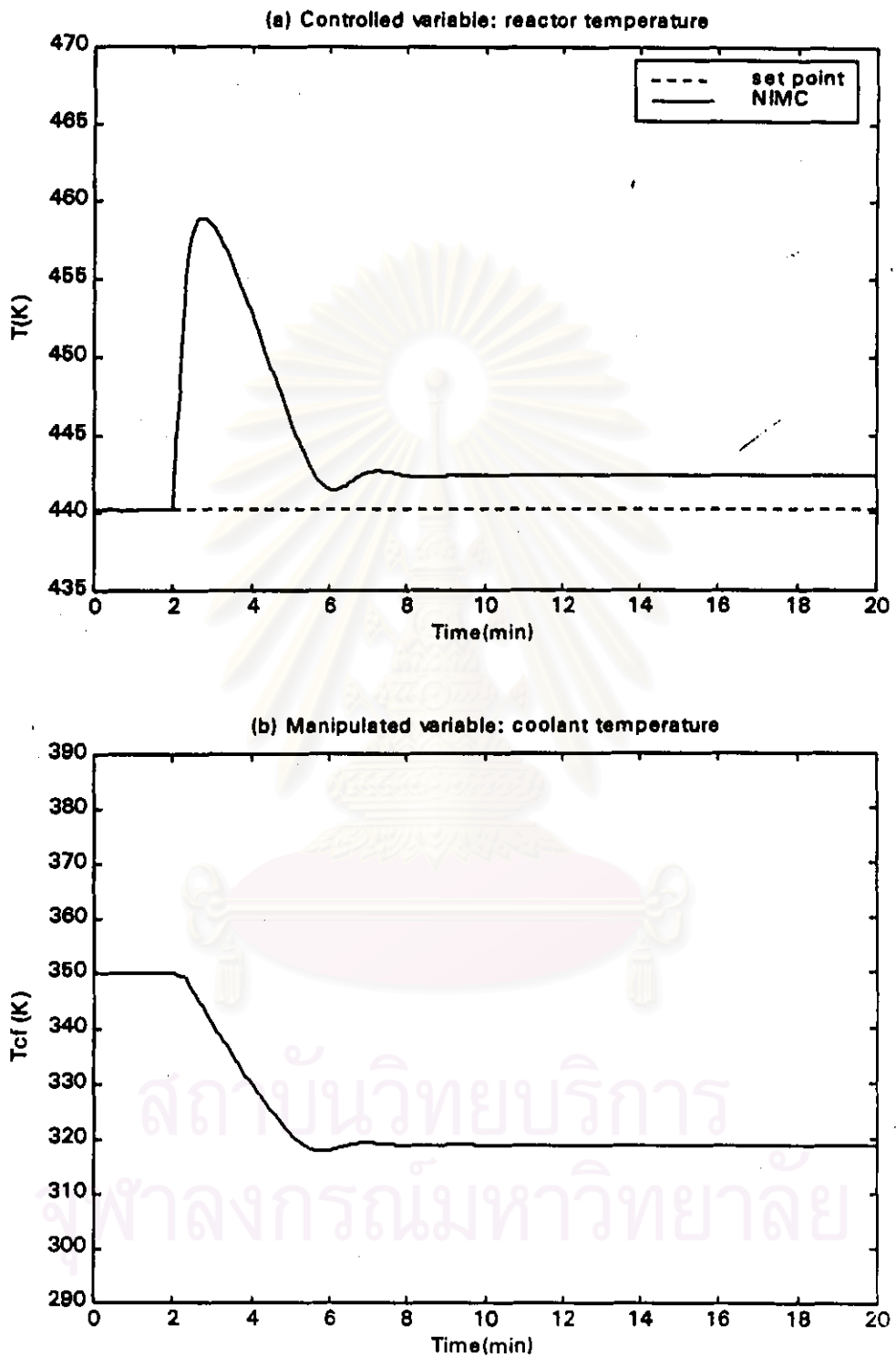
Figure 7.11: Disturbance rejection test with NIMC.

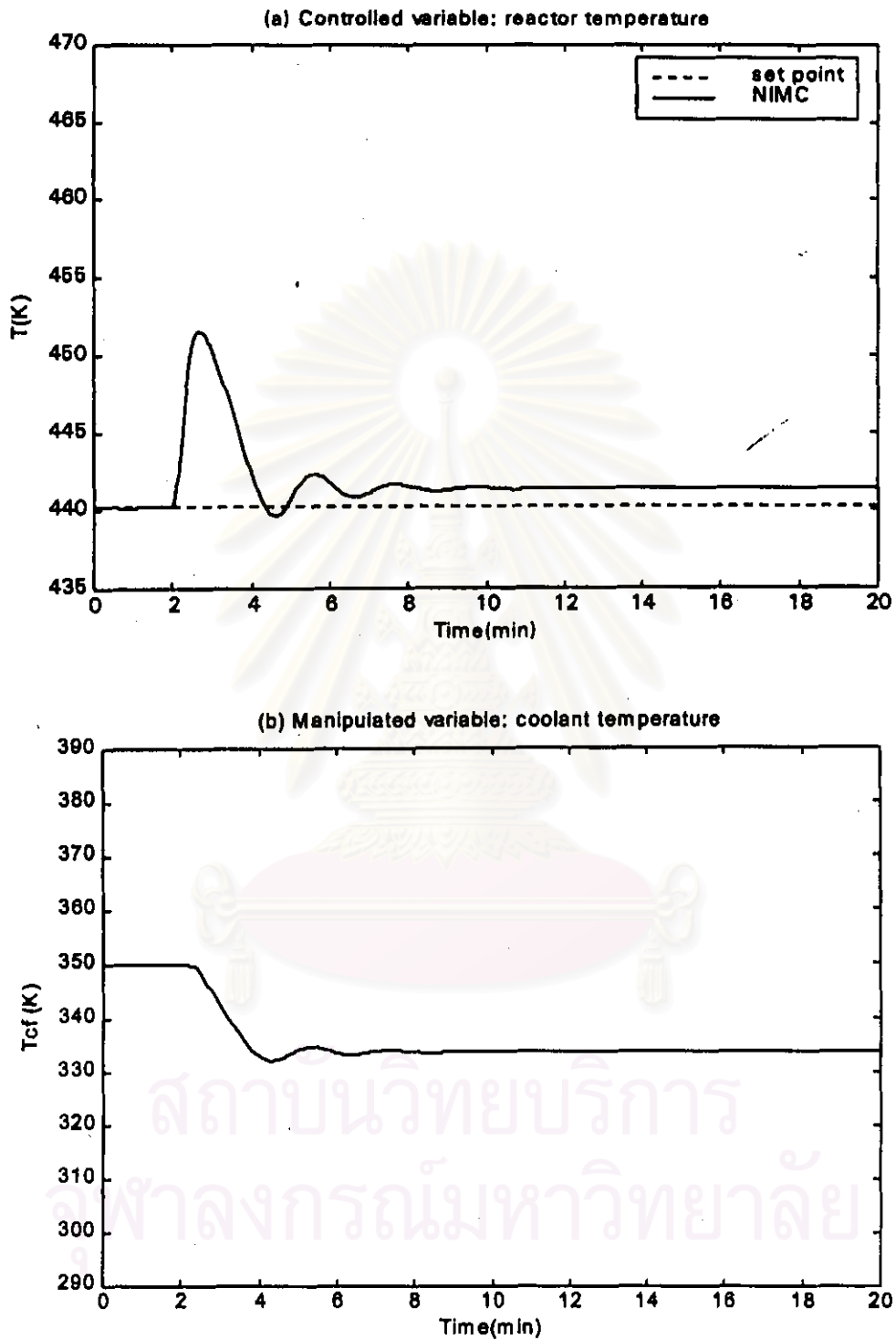Response to 10% load disturbance of the measured feed temperature

Figure 7.12: Disturbance rejection test with NIMC.

Response to 10% load disturbance of the unmeasured feed concentration
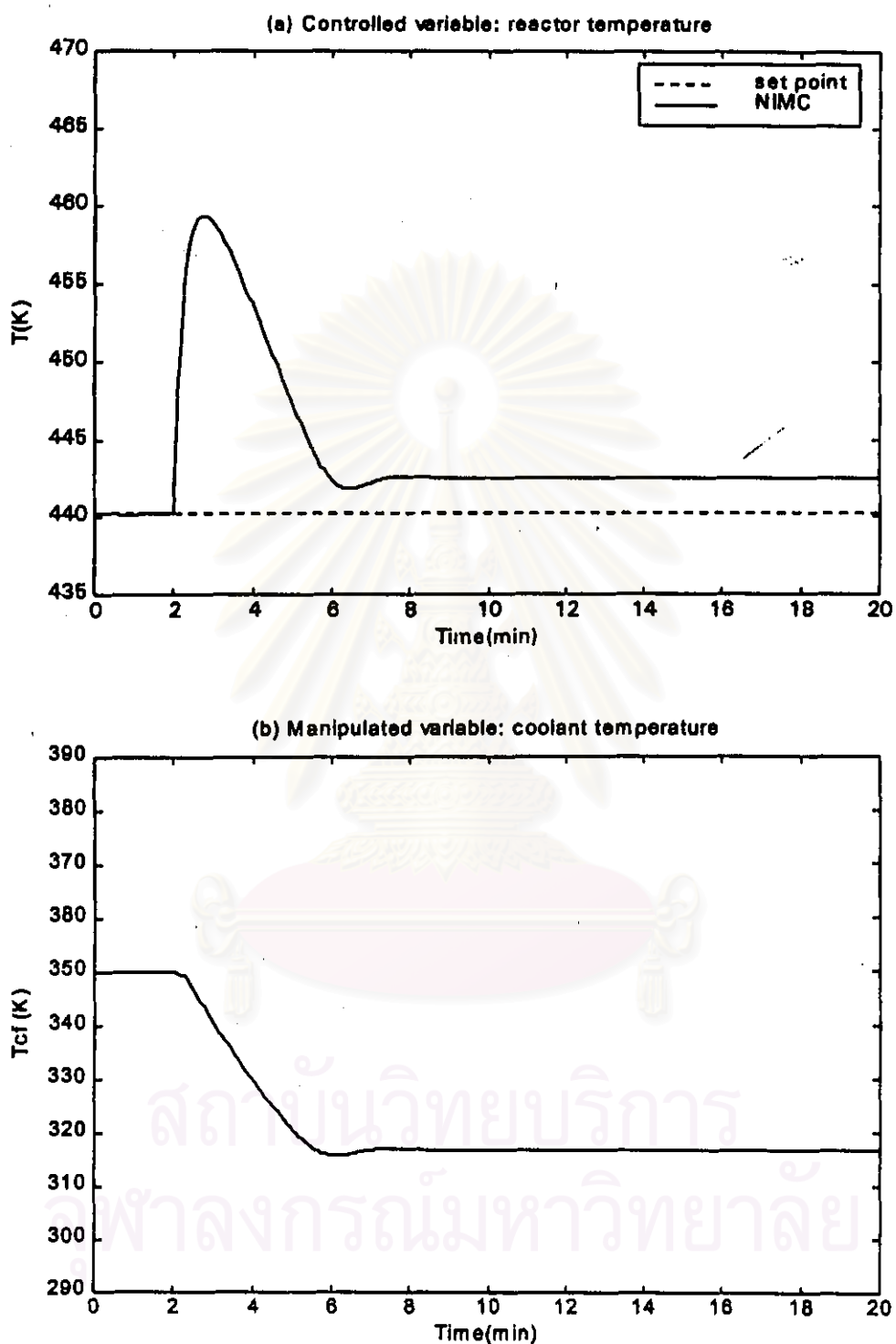
Figure 7.13: Disturbance rejection and robustness tests with NIMC.
Response to 10% load disturbance in the measured feed temperature and
20% model error in the pre-exponential constant

(a) Controlled variable: reactor temperature

(b) Manipulated variable: coolant temperature

Figure 7.14: Disturbance rejection and robustness tests with NIMC. Response to

10% load disturbance in the unmeasured feed concentration and

20% model error in the pre-exponential constant

Figure 7.15: Disturbance rejection and robustness tests with NIMC. Response to

10% load disturbance in the measured feed temperature and

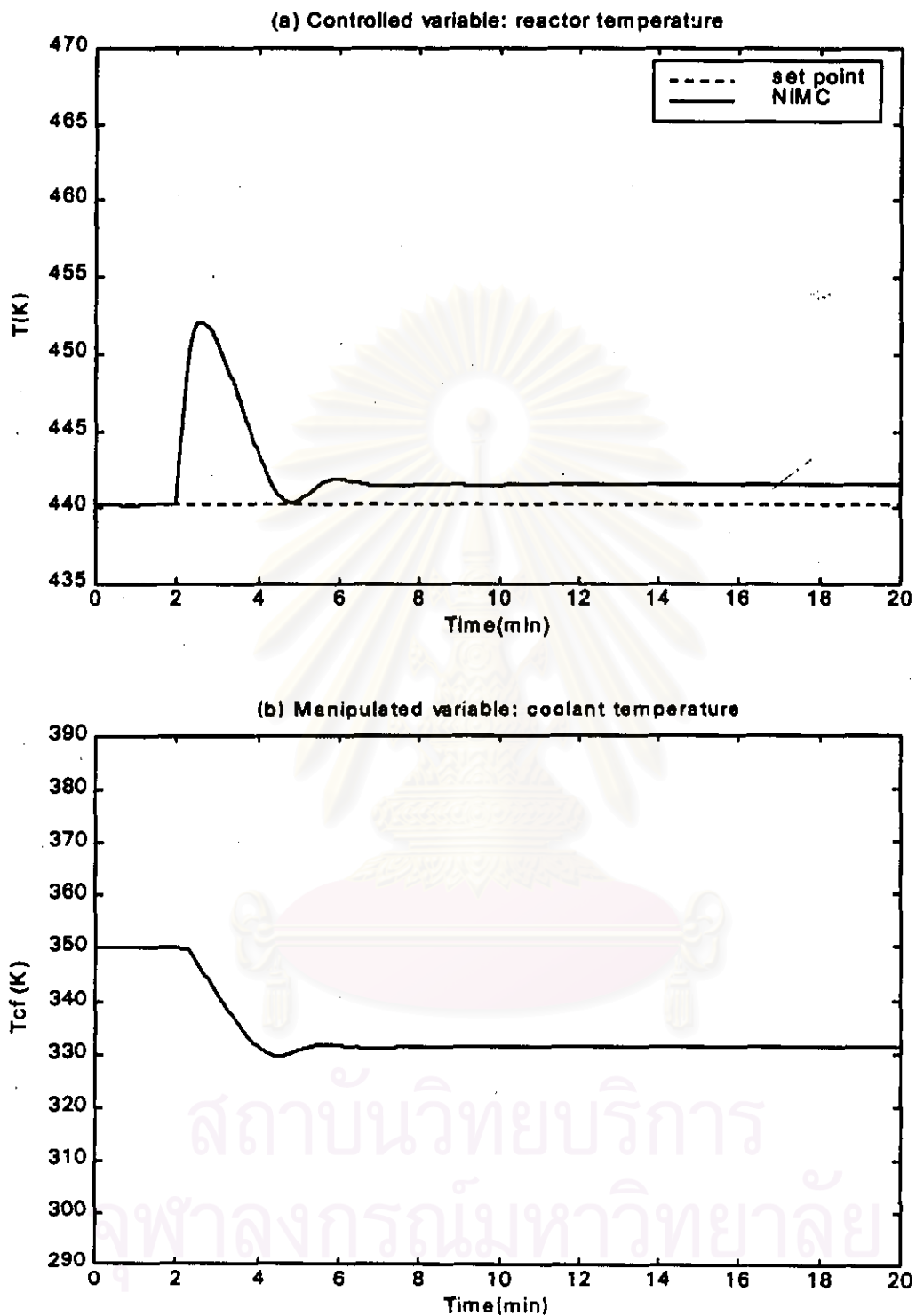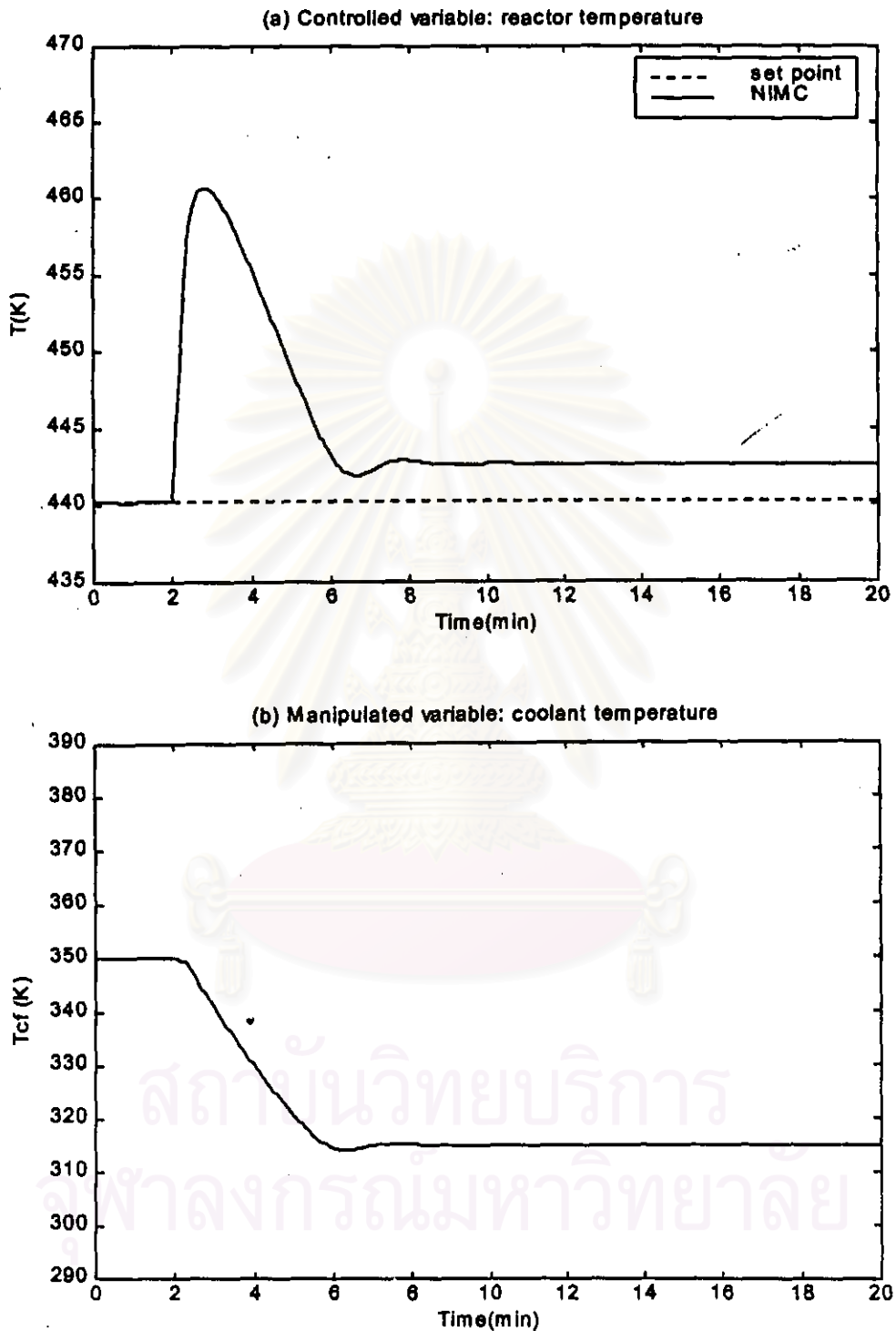-50% model error in the heat transfer coefficient

Figure 7.16: Disturbance rejection and robustness tests with NIMC. Response to

10% load disturbance in the unmeasured feed concentration and

-50% model error in the heat transfer coefficient

Figure 7.17: Disturbance rejection and robustness tests with NIMC.
Response to 10% load disturbance in the measured feed temperature and
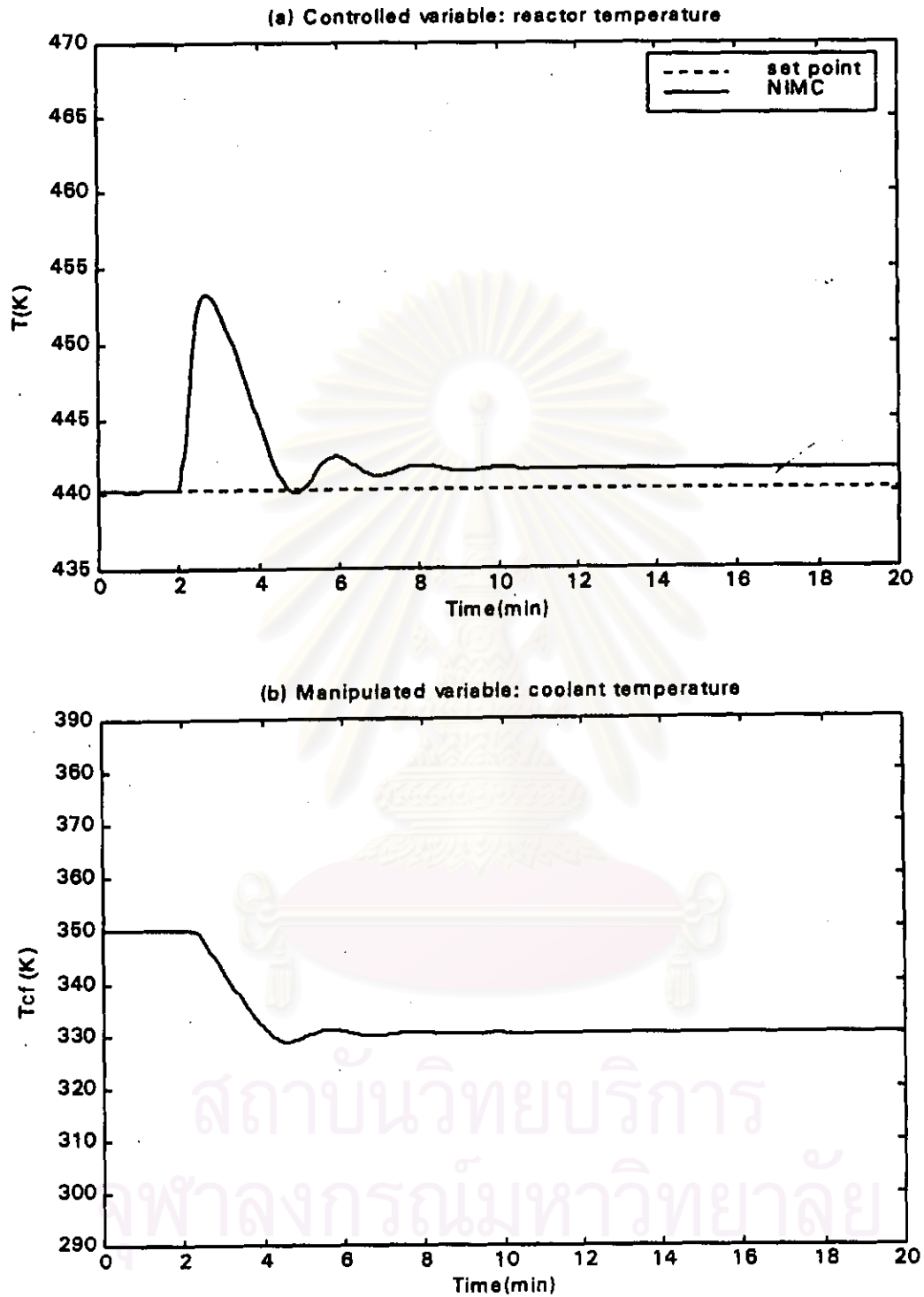10% model error in the heat of reaction
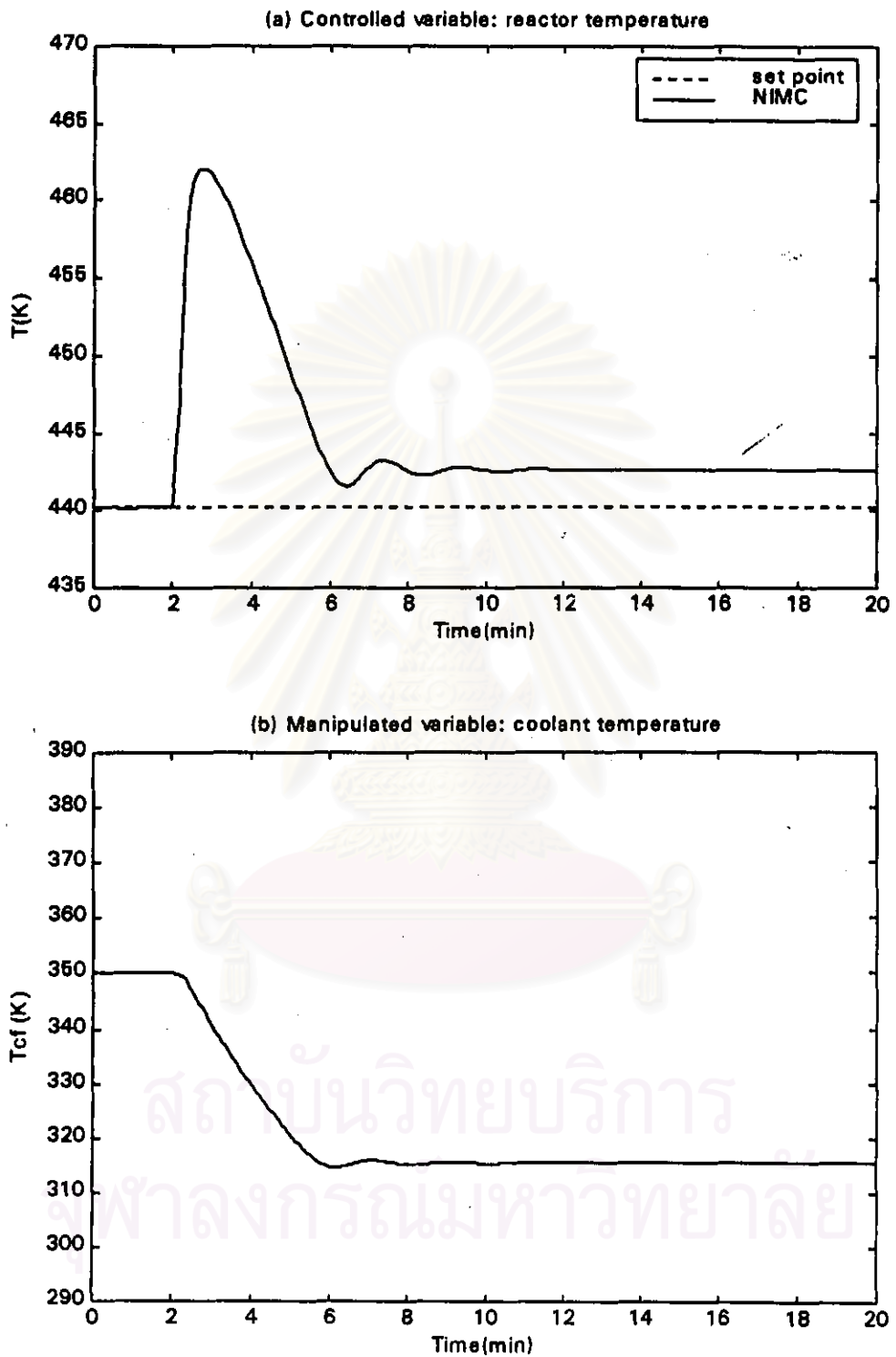
Figure 7.18: Disturbance rejection and robustness tests with NIMC.
Response to 10% load disturbance in the unmeasured feed concentration and
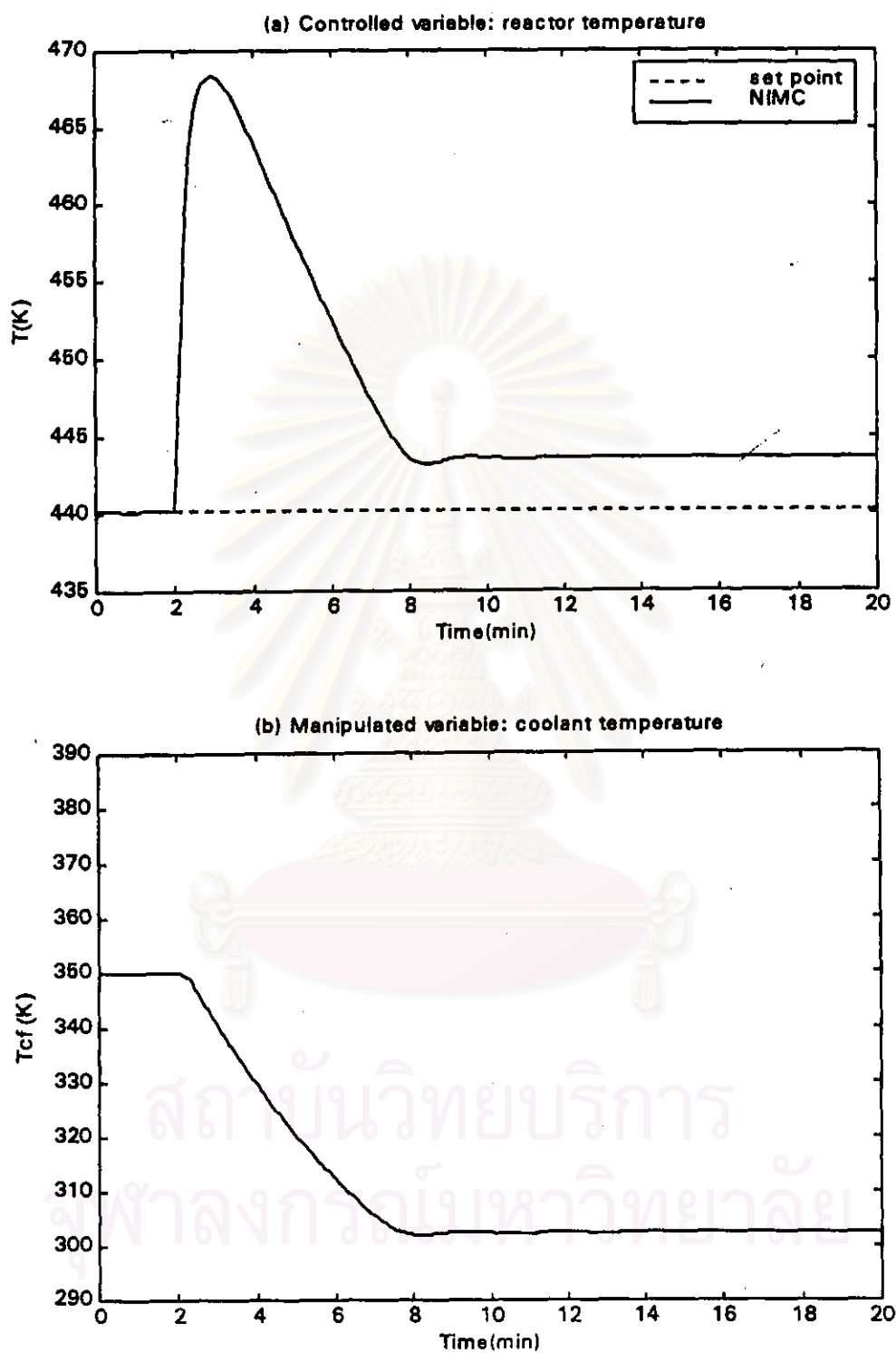10% model error in the heat of reaction
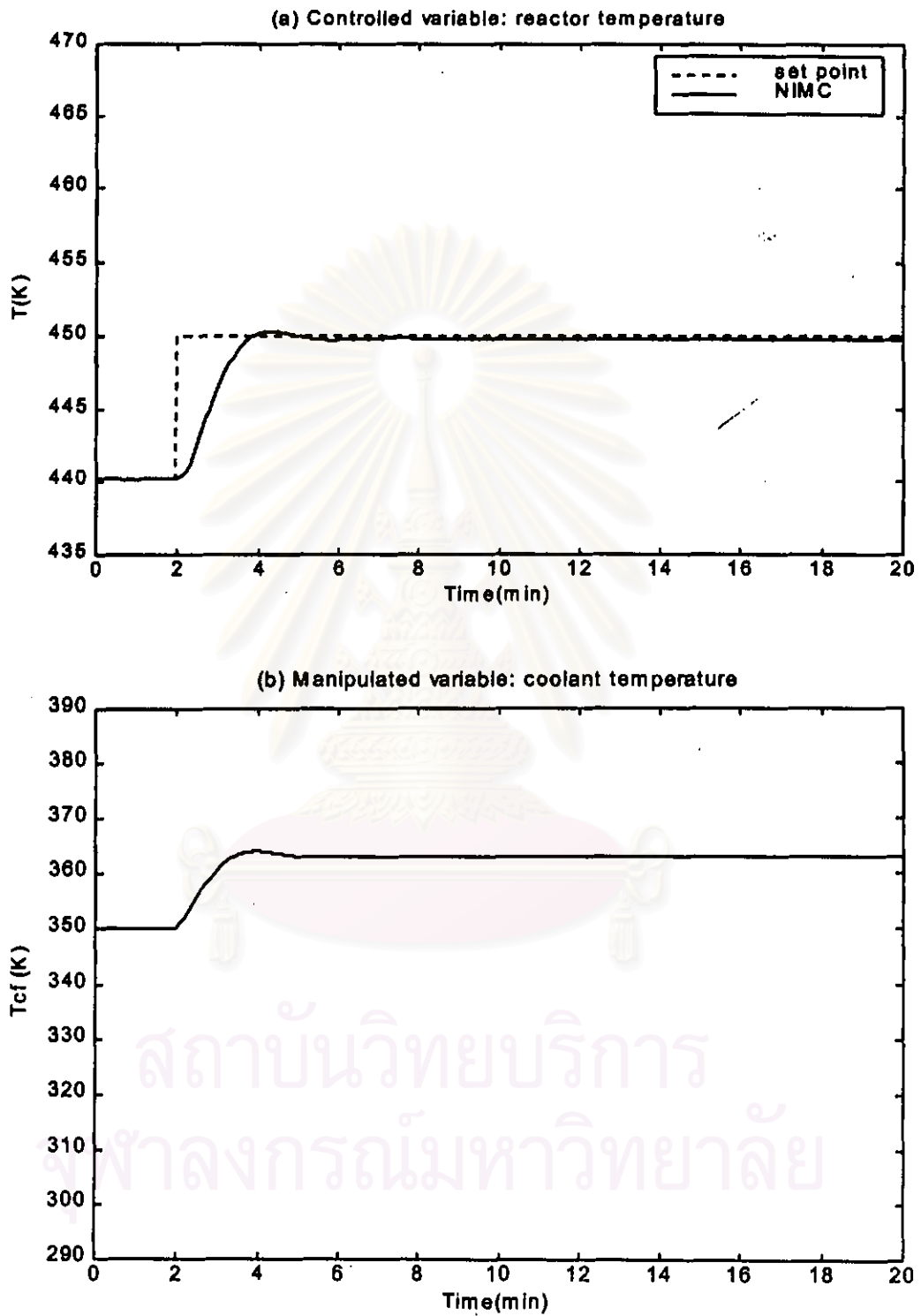
Figure 7.19: Set point tracking test with NIMC

Response to set point change from 440.2 K to 450 K

(a) Controlled variable: reactor temperature

(b) Manipulated variable: coolant temperature

Figure 7.20: Set point tracking and robustness tests with NIMC

Response to set point change from 440.2 K to 450 K and

20% model error in the pre-exponential constant
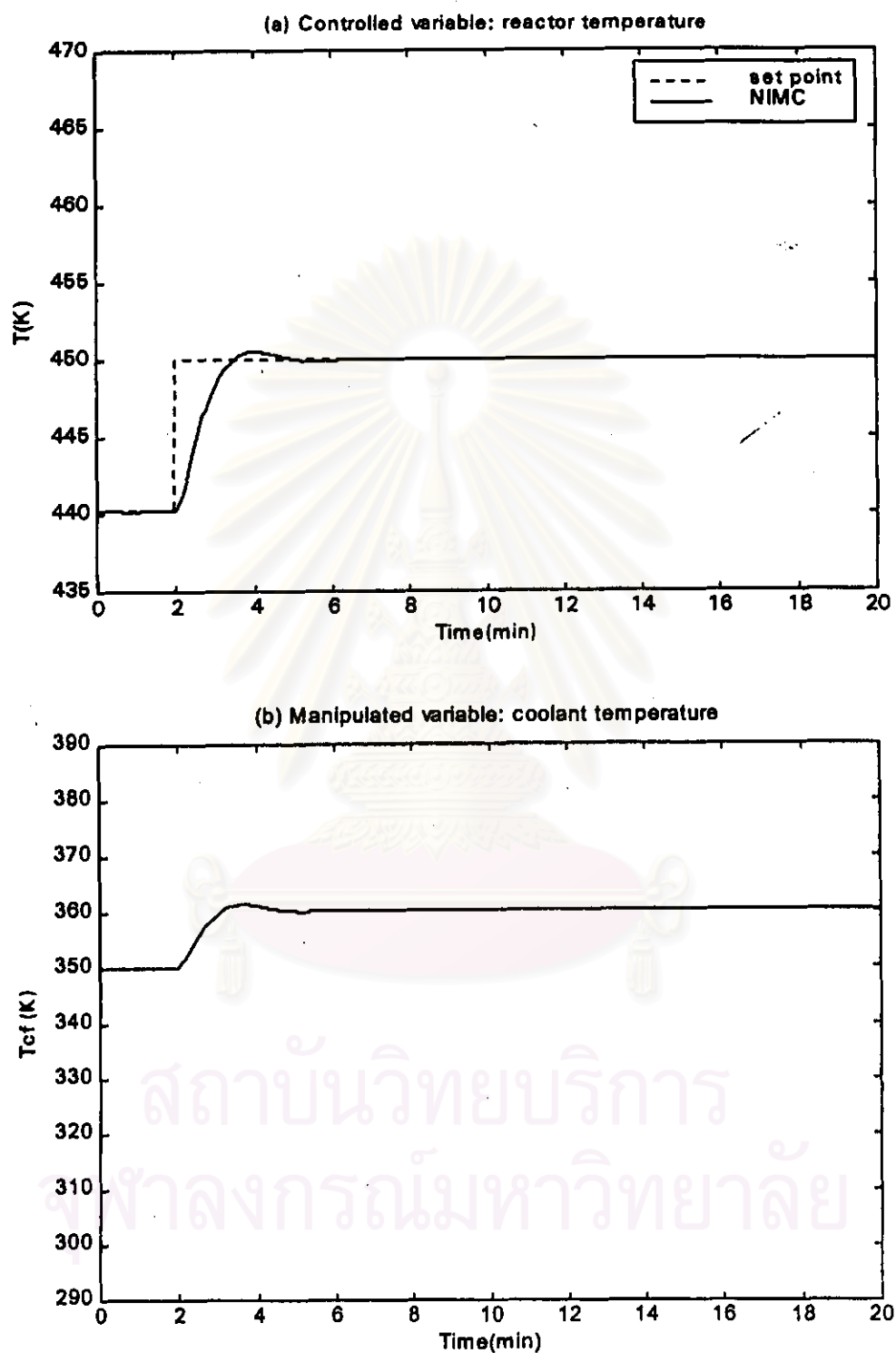
Figure 7.21: Set point tracking and robustness tests with NIMC

Response to set point change from 440.2 K to 450 K and

-50% model error in the heat transfer coefficient
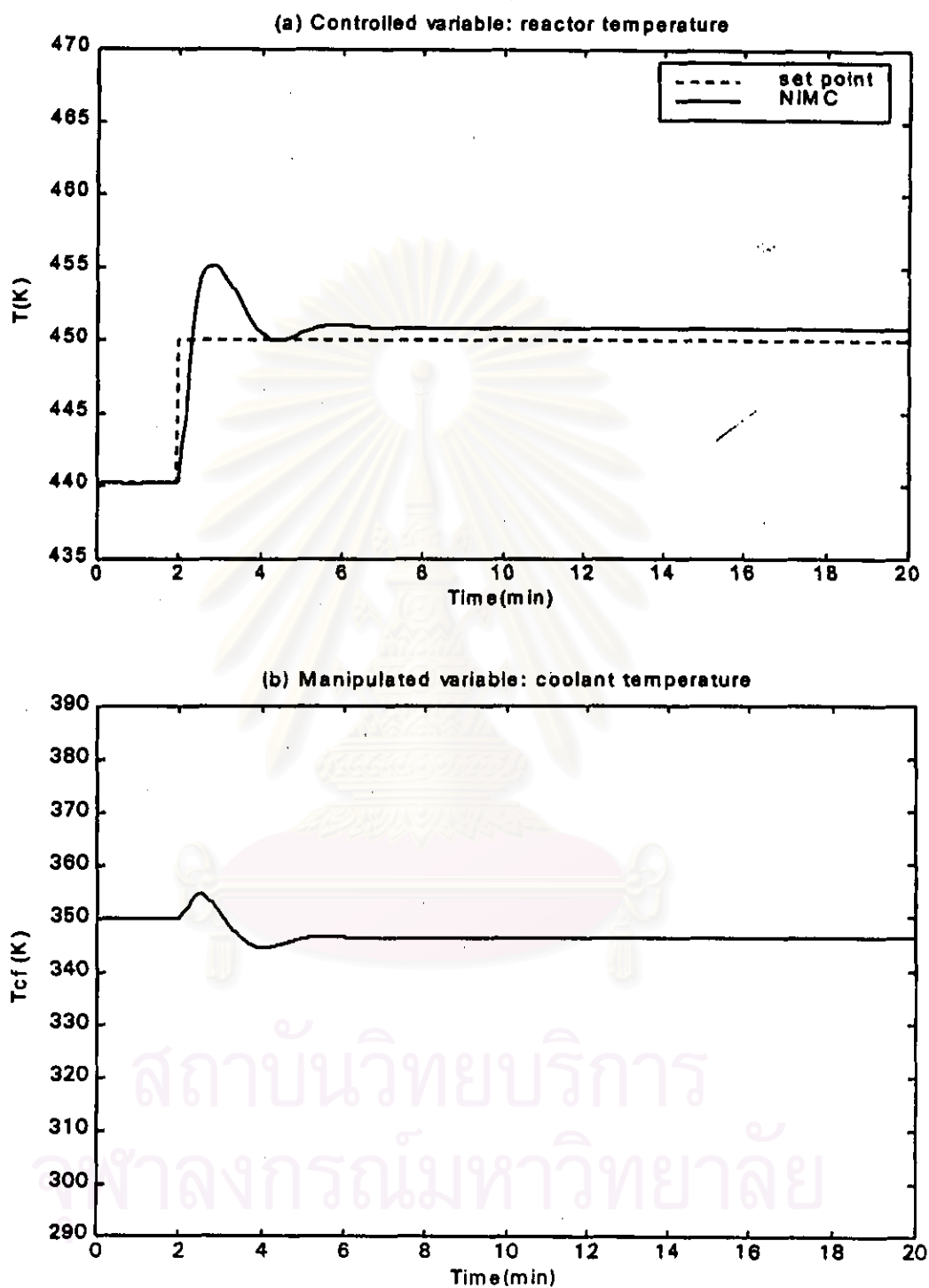
Figure 7.22: Set point tracking and robustness tests with NIMC

Response to set point change from 440.2 K to 450 K and

10% model error in the heat of reaction

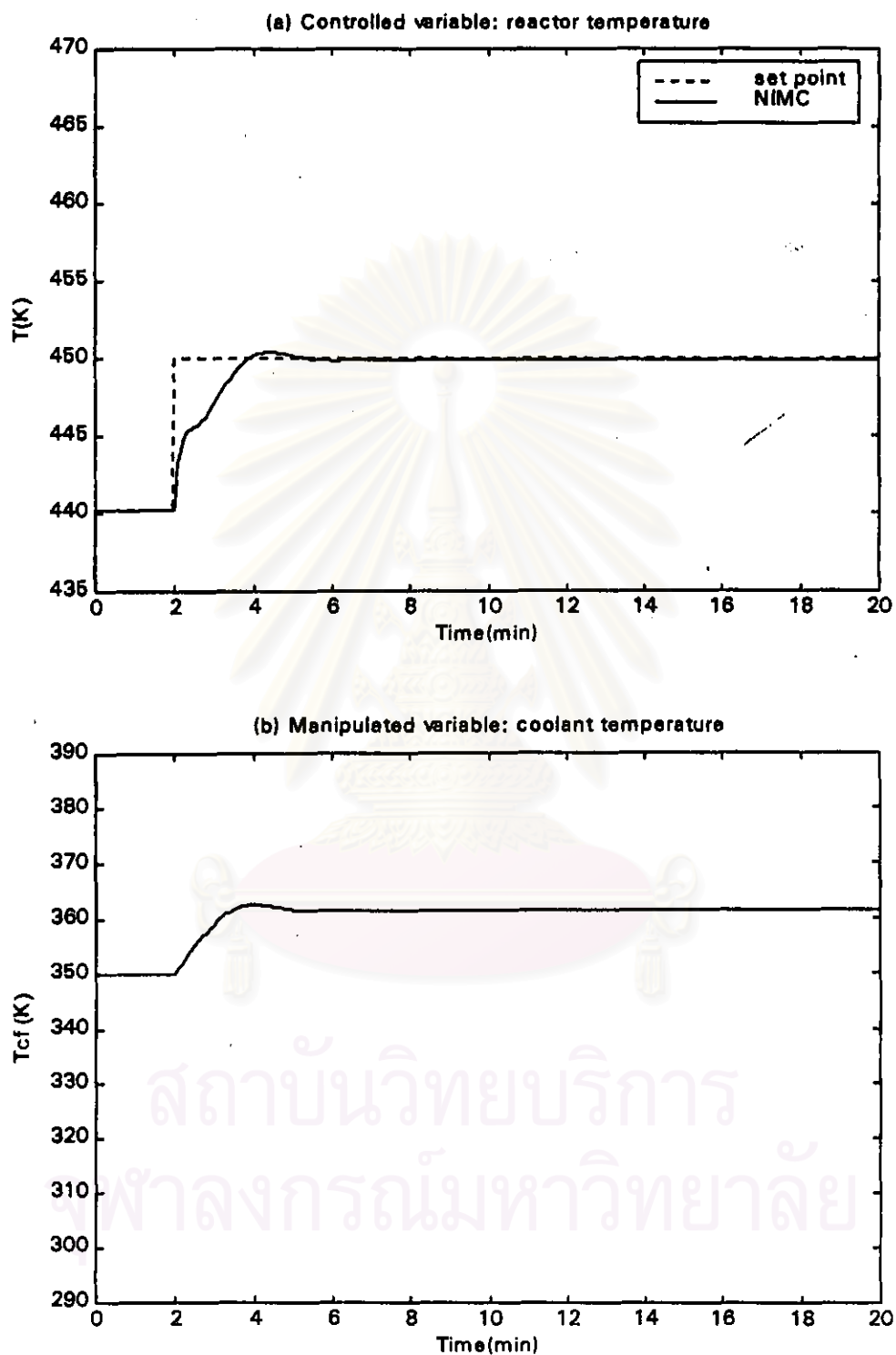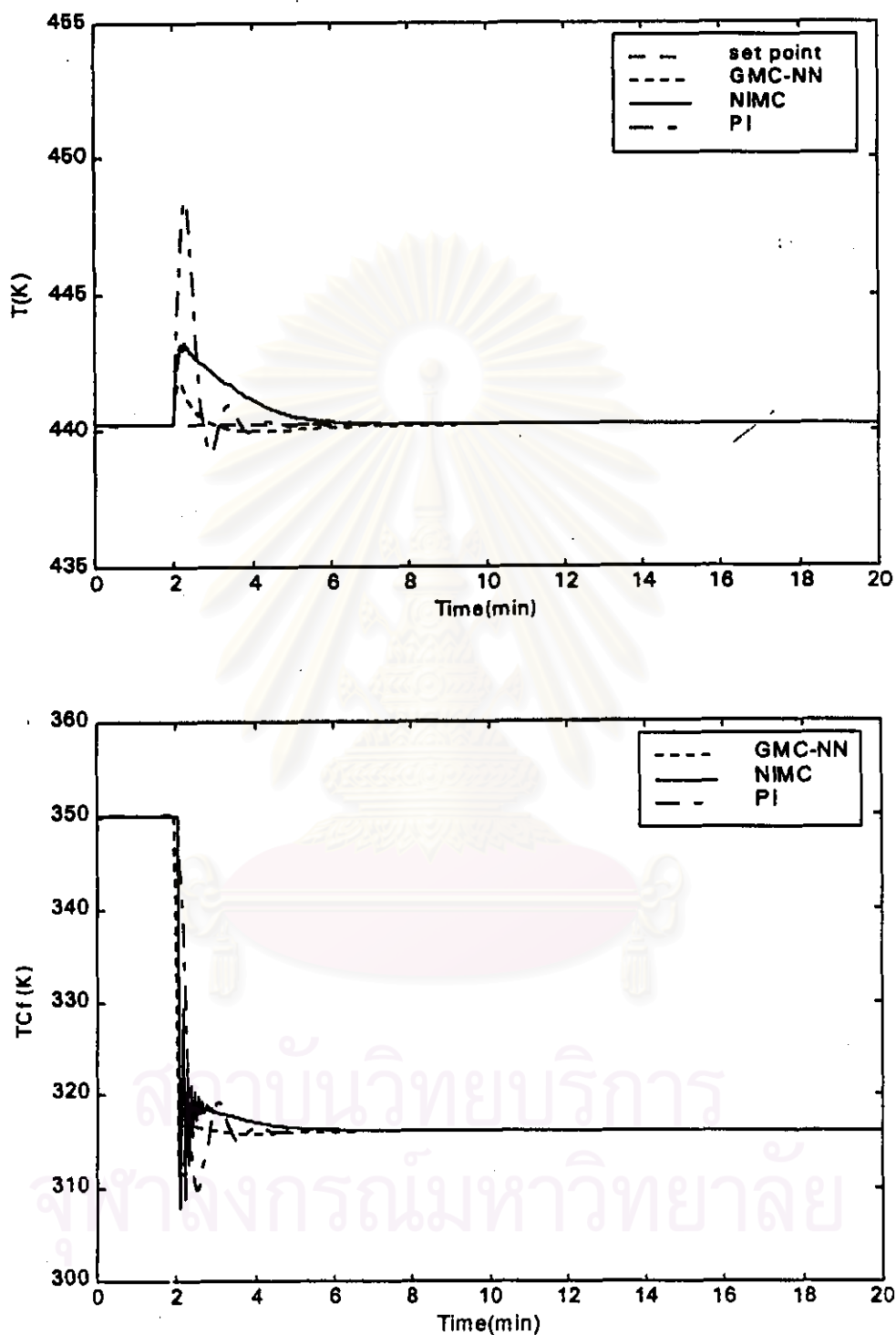Figure 7.23: Control performance of the GMC-NN, NIMC (with PI), and PI control

Response to 10% load disturbance in the measured feed temperature

Controlled variable (upper) and manipulated variable (lower)
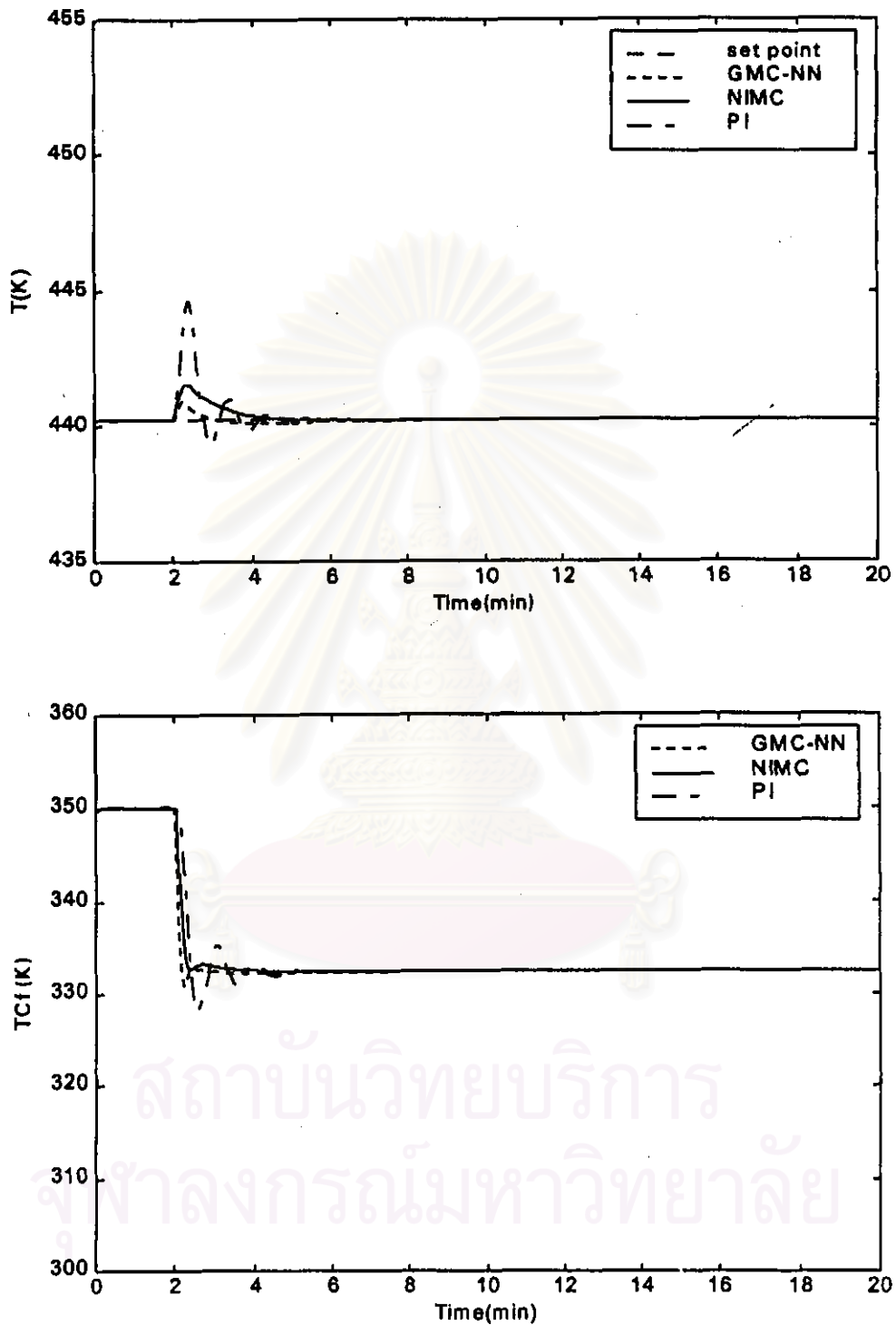
Figure 7.24: Control performance of the GMC-NN, NIMC (with PI), and PI control.

Response to 10% load disturbance in the unmeasured feed concentration

Controlled variable (upper) and manipulated variable (lower)
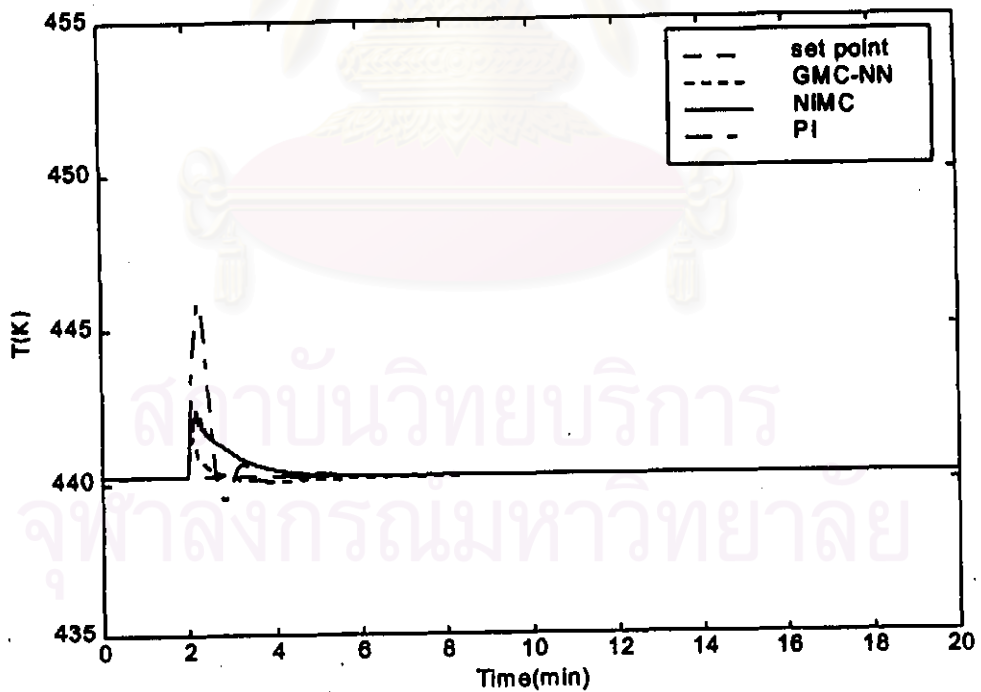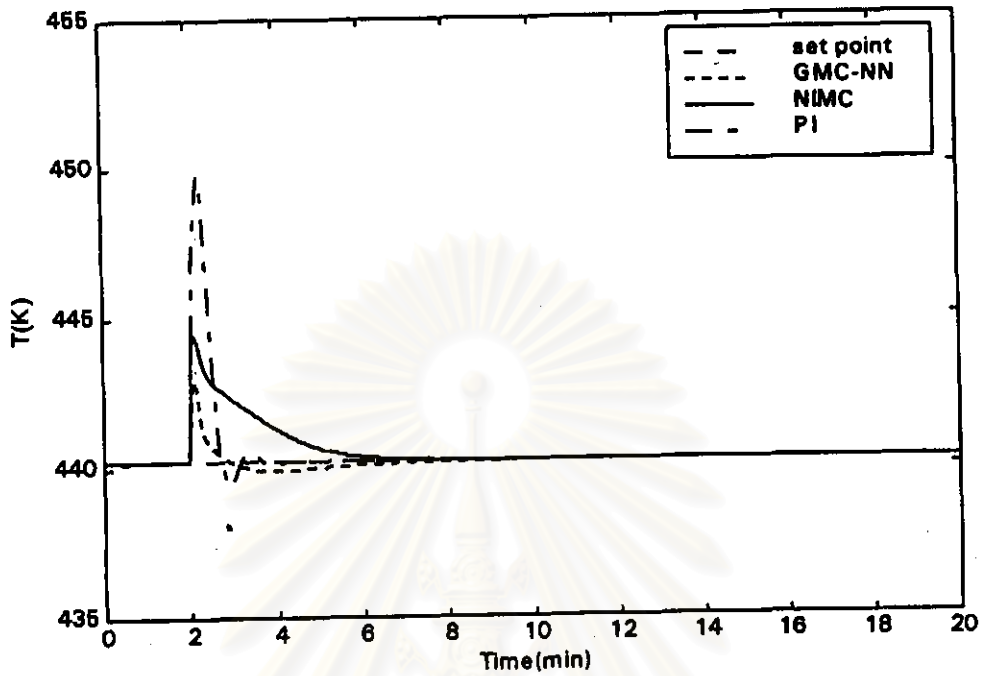
Figure 7.25: Control performance of the GMC-NN, NIMC (with PI), and PI control.

Response to 20% model error in the pre-exponential constant and

(upper) 10% load disturbance in the measured feed temperature

(lower) 10% load disturbance in the unmeasured feed concentration
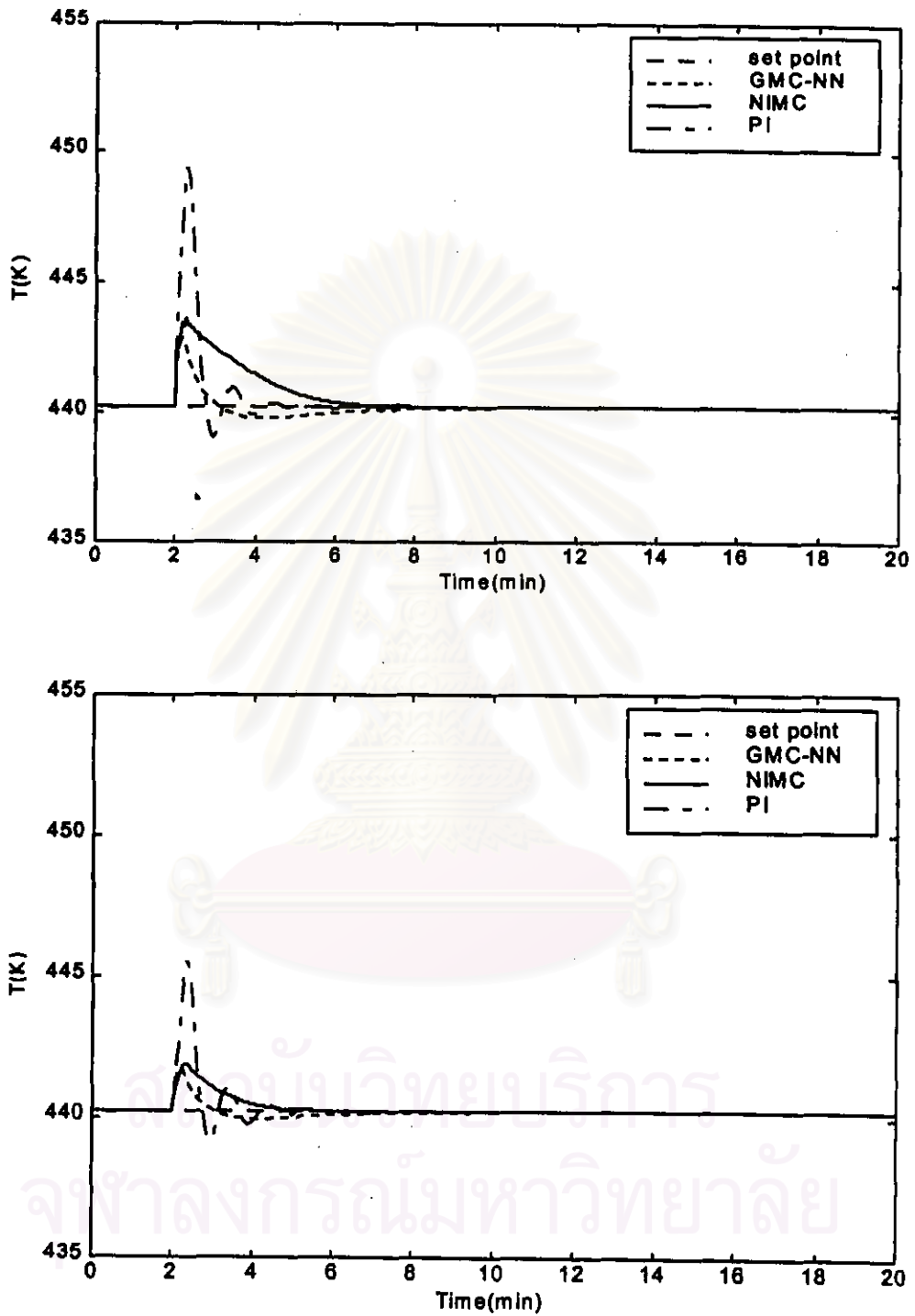
Figure 7.26: Control performance of the GMC-NN, NIMC (with PI), and PI control.
Response to -50% model error in the heat transfer coefficient and
(upper) 10% load disturbance in the measured feed temperature
(lower) 10% load disturbance in the unmeasured feed concentration
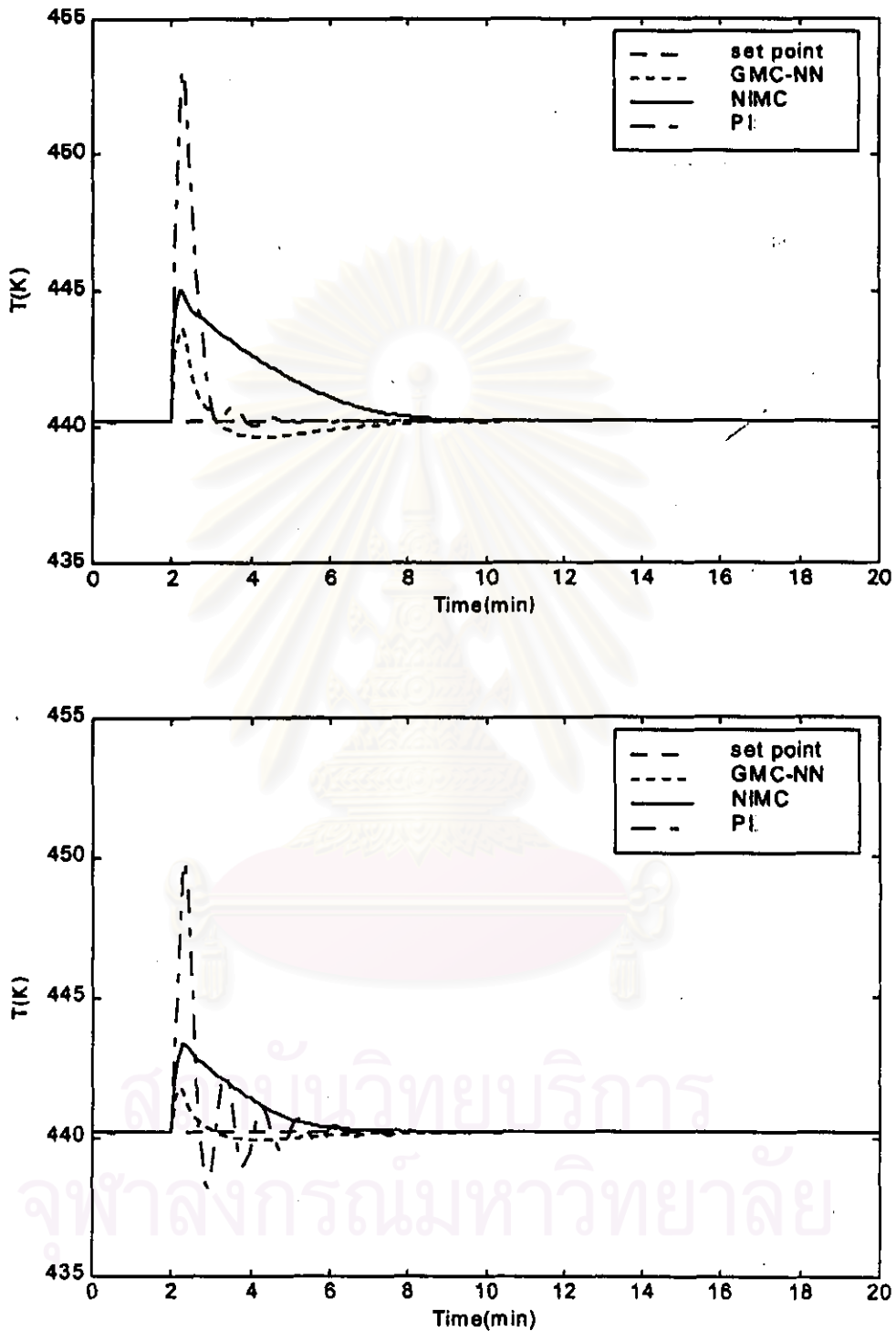
Figure 7.27: Control performance of the GMC-NN, NIMC (with PI), and PI control.

Response to 10% model error in the heat of reaction and

(upper) 10% load disturbance in the measured feed temperature

(lower) 10% load disturbance in the unmeasured feed concentration

Figure 7.28: Control performance of the GMC-NN, NIMC (with PI), and PI control.

Response to set point change from 440.2 K to 450 K and

(upper) nominal case

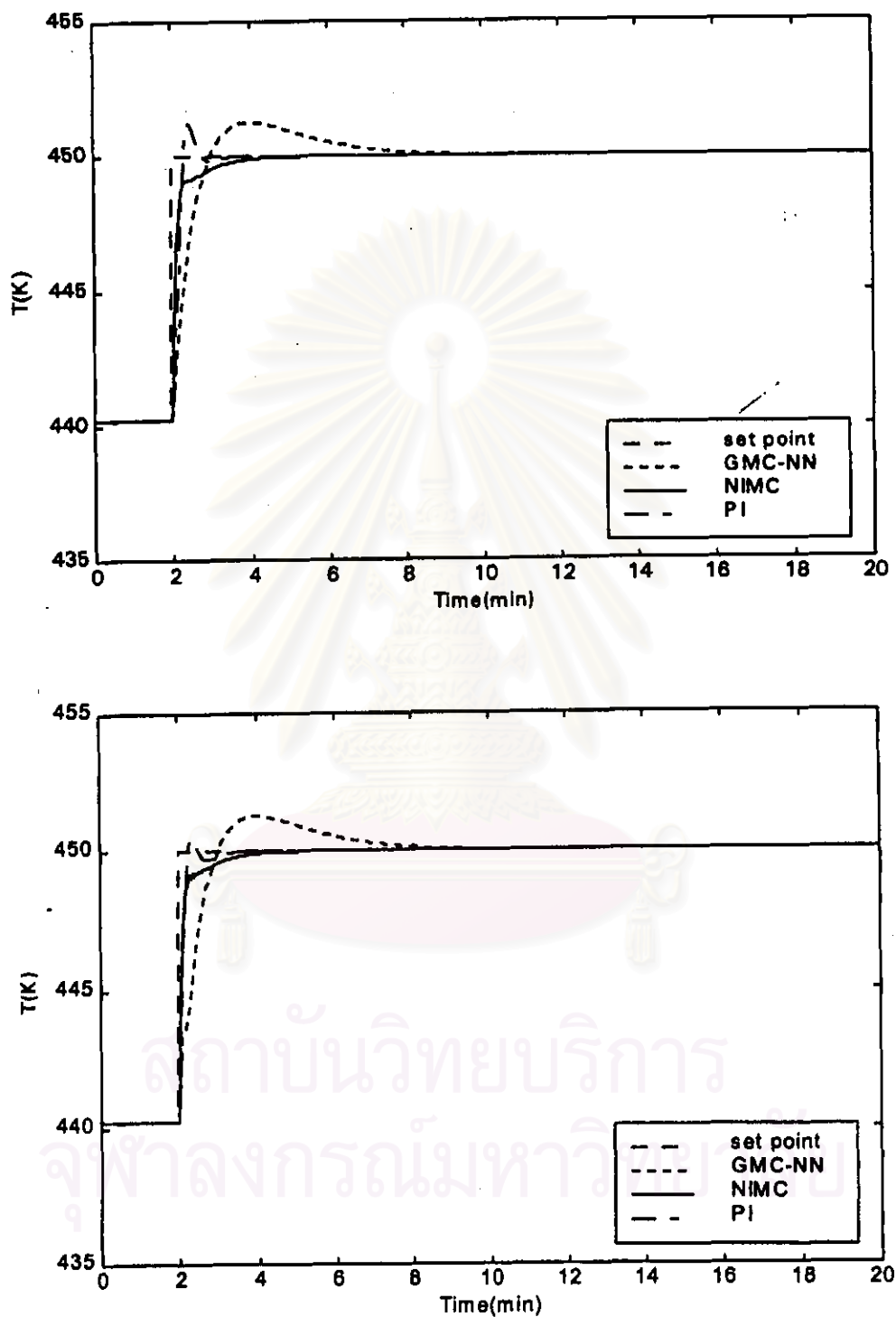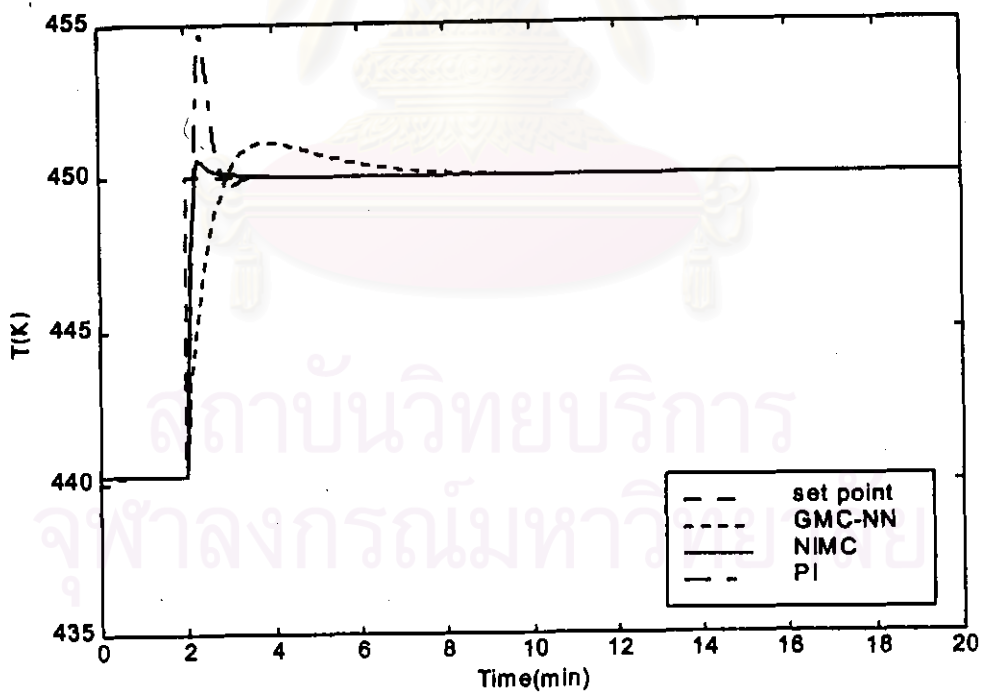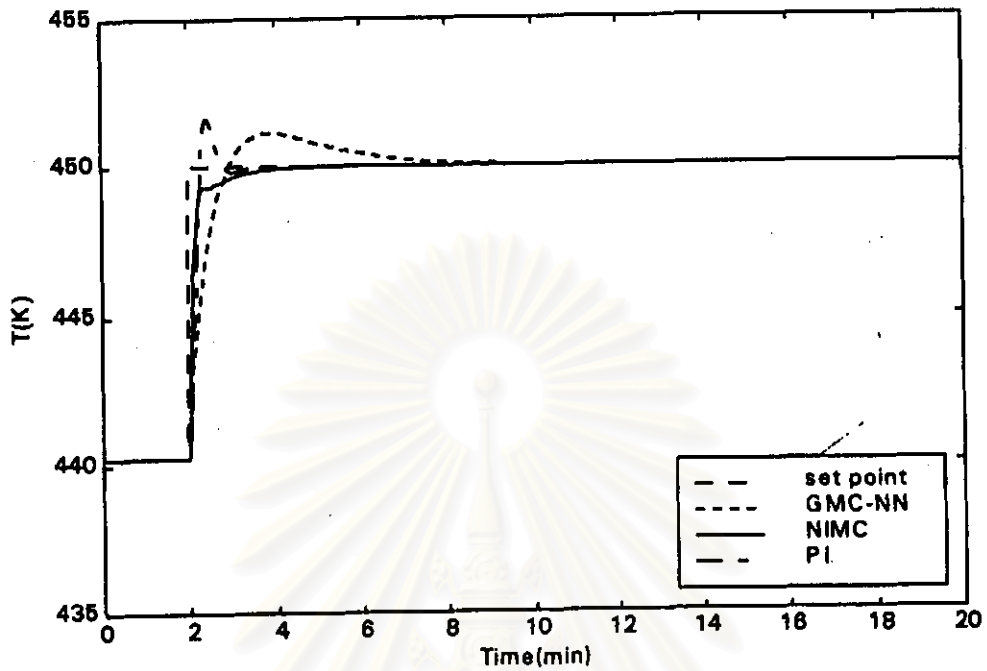(lower) 20% model error in the pre-exponential constant

Figure 7.29: Control performance of the GMC-NN, NIMC (with PI), and PI control.

Response to set point change from 440.2 K to 450 K and

(upper) -50% model error in the heat transfer coefficient

(lower) 10% model error in the heat of reaction

7.4   Results and Discussions

In this chapter the NIMC configuration is utilized to control the reactor temperature (T) by manipulating the coolant feed temperature (T_{cf}). Performance tests and robustness tests are carried out in order to investigate the control performances of the control system. The performance tests are classified into disturbance rejection and set point tracking. For the study on the disturbance rejection, it is composed of 10% change of the feed temperature (T_f) and 10% change of the feed concentration (C_{Af}) from the nominal value. For the study on set point tracking, the desired set point is shifted from its nominal value (440.2 K) to 450 K. The robustness tests are divided into the presence of the plant-model mismatches of the process parameters: 20% change of the Arrhenius pre-exponential constant (k_o), -50% change of the heat transfer coefficient (hA), and 10% change of the heat of reaction ($-\Delta H$). (Note that every change occurs at t=2 min.) All changes studied in this chapter are explored in the directions that cause to the increase of the reactor temperature from its desired set point.

The neural network structure representing the forward model of the CSTR is depicted in Figure 7.1. Figure 7.2 to Figure 7.4 illustrate the simulation results obtained from neural network forward modeling of CSTR for training, cross validation and testing data set. They indicate that the selected neural network can learn the forward dynamics of the system successfully. In the aspect of inverse modeling, the selected neural network, representing the inverse model of the CSTR is shown in Figure 7.5 can also learn the inverse dynamics of the system as demonstrated in Figure 7.6 to Figure 7.8.

Firstly, the control system is tested with 10% change of the feed temperature in the nominal condition, it can be seen in Figure 7.11 that the reactor temperature is increased from the desired set point (440.2 K) to 459 K within 1 minute after the system is disturbed. As the result, the NIMC generates the controlled signal, the coolant feed temperature, below its nominal value (from 350 K to 319 K) in order to bring the reactor temperature to its desired set point again. Due to the decrease of the

coolant feed temperature, the reactor temperature is dropped and maintained at 442.5 K after t=9 min. That means the controller generates 2.3 K offsets above the desired set point.

Secondly, 10% change of the feed concentration in the nominal condition is the other test employed to evaluate the control performance. It can be seen that the reactor temperature is enhanced to 452 K and then decreased with some oscillation, due to the decrease of the coolant feed temperature (from 350 K to 334 K). After that it is kept constant at 441 K after t=11 min whereas small offset (0.8 K) control performance exists as illustrated in Figure 7.12.

Thirdly, the system is disturbed with 10% change of the feed temperature in the presence of the plant-model mismatch of the Arrhenius pre-exponential constant. The result obtained is depicted in Figure 7.13. The reactor temperature response is similar to that obtained in case of the change in feed temperature in nominal condition (Figure 7.11) but with larger overshoot. That is the reactor temperature is raised to 459.5 K. Then it is dropped and maintained constant at 442.5 K because of the decrease in the coolant feed temperature from 350 K to 317 K. Equal offset performance compared to that of the first case is obtained

Next, the control system is tested with the change in the feed concentration in the presence of the plant-model mismatch as well as that of the previous case. It can be seen that the reactor temperature is enlarged from 440.2 K to 452 K. After that it is decreased and kept constant at 441.5 K. While the coolant feed temperature is changed from 350 K to 332 K. Small offset (1.3 K) performance is obtained as shown in Figure 7.14.

In the presence of plant-model mismatch of the heat transfer coefficient, the control system is tested in the same manner as that of the Arrhenius pre-exponential constant. Figure 7.15 demonstrates the response of the reactor temperature and the coolant feed temperature due to the feed temperature disturbance while Figure 7.16 illustrates the results caused from the change in the feed concentration. In Figure 7.15, the reactor temperature is increased from 440.2 K to 461 K. Because of the decrease

in the coolant feed temperature (from 350 K to 315 K), the reactor temperature is lowered to 442.5 K. Finally, offset performance with 2.3 degree above the desired set point is obtained. In Figure 7.16, the reactor temperature is raised from 440.2 K to 453.5 K and it is then decreased, by the change of the coolant feed temperature from 350 K to 330.2 K, and kept constant at 441.5 K. As the result, 1.3 degree offset performance is noticed.

Same performance tests are still conducted to the control system in the presence of the plant-model mismatch in the heat of reaction. Figure 7.17 and Figure 7.18 demonstrates the control performance of the NIMC when the system is disturbed with the change in the feed temperature and the feed concentration, respectively. In Figure 7.17, it can be seen that the reactor temperature is enhanced to 468.5 K. It is then reduced to 443.5 K, in spite of the change in the coolant feed temperature from 350 K to 302 K. That means offset performance with 3.3 K above its desired set point is generated. In Figure 7.18, the reactor temperature is raised to 462 K and then reduced to 442.5 K despite the change in the coolant feed temperature from 350 K to 315.5 K. In addition, 2.3 K offset performance is produced.

Next, the control system is tested with set point tracking. In nominal condition, the reactor is gradually increased to the new desired set point with small overshoot. Then it is reduced and maintained constant, nearly the new desired set point with minimal offset as depicted in Figure 7.19.

When the set point tracking is performed in the presence of plant-model mismatch of the Arrhenius pre-exponential constant, minimal offset performance below the new desired set point can be seen in Figure 7.20. While the coolant feed temperature is decreased to 362 K. On the other hand, offset-free performance is obtained as illustrated in Figure 7.21 for the presence of plant-model mismatch of the heat transfer coefficient. In this case, the coolant feed temperature is changed from 350 K to 360.1 K. However 1 K offset performance is obtained in case of the presence of plant-model mismatch in the heat of reaction as shown in Figure 7.22.

In summary, minimal offset or offset-free performances are obtained from the set point tracking test in either nominal condition or plant-model mismatches. Nevertheless, some offsets still exist in the control performance when the system is tested with disturbance rejection. These may cause from the existence of model errors and the lack of the exact inverse model. Consequently, the PI controller is placed in series after the NN controller in order to remove those offsets. As the result, offset-free performances are obtained in every case study. The results are then compared to those of the GMC-NN and PI controllers. The Integral Absolute Error (IAE) is used as a performance index to indicate the quantitative efficiency of each control system as given in Table 7.1.

With disturbance tests in nominal case and in the presence of plant-model mismatch, the order of the control performance arranged from the best to the worst control performance is that of the GMC-NN, the NIMC-PI, and the PI controller. Overshoot performances without oscillation are obtained from the GMC-NN and the NIMC-PI control whereas large overshoot performance with oscillation is produced in the PI control. In comparison to the disturbances caused from the change in the feed temperature and the feed concentration, each control system give higher overshoot against the disturbance of the feed temperature. Figure 7.23 to Figure 7.24 demonstrate the control performance of the each control system with the disturbance rejection tests due to the change in the feed temperature and the feed concentration in nominal condition, respectively. Furthermore the control performances of each control system, when the system is tested with disturbance rejection in the presence of the plant-model mismatch in the Arrhenius pre-exponential constant, the heat transfer coefficient, and the heat of reaction, are illustrated in Figure 7.25 to Figure 7.27, respectively.

For set point tracking test, in nominal condition the GMC-NN and the PI control produce comparable overshoot but the PI control can lead the system to its desired set point faster than the GMC-NN. However, the NIMC-PI control can control the reactor temperature at new set point faster than the GMC-NN but slower than the PI control. The results obtained are shown in Figure 7.28.

For set point tracking test in the presence of plant-model mismatch in the Arrhenius pre-exponential constant as depicted in Figure 7.28, it can be seen that the PI control generates lower overshoot compared to that of the GMC-NN. While the NIMC-PI give the same control performance as that in the nominal condition but with some small oscillation.

Next, the system is tested with set point tracking in the presence of plant-model mismatch in the heat transfer coefficient, the PI control produce higher overshoot compared to that of the GMC-NN. While the NIMC-PI control can control the reactor temperature at new set point without overshoot as illustrated in Figure 7.29.

Finally, with set point tracking test in the presence of plant-model mismatch in the heat of reaction, the PI control produces large overshoot while the GMC-NN and the NIMC give some overshoot before they lead the reactor temperature to new set point as shown in Figure 7.29.

For the quantitative control performance of three control systems: GMC-NN, NIMC-PI, and PI controls are also considered in term of the IAE. The GMC-NN control gives the best control performance followed by the NIMC-PI and the PI controls in case of disturbance rejection tests in nominal condition and in the presence of plant-model mismatch. In addition, the NIMC-PI is superior to the PI control when the system is disturbed with unmeasured concentration in both nominal condition and the presence of plant-model mismatches. However with set point tracking test in nominal condition and in the presence of the plant-model mismatches, the NIMC-PI control gives the best control performance among those control systems.